

FACULTY OF SCIENCE
UNIVERSITY OF COPENHAGEN

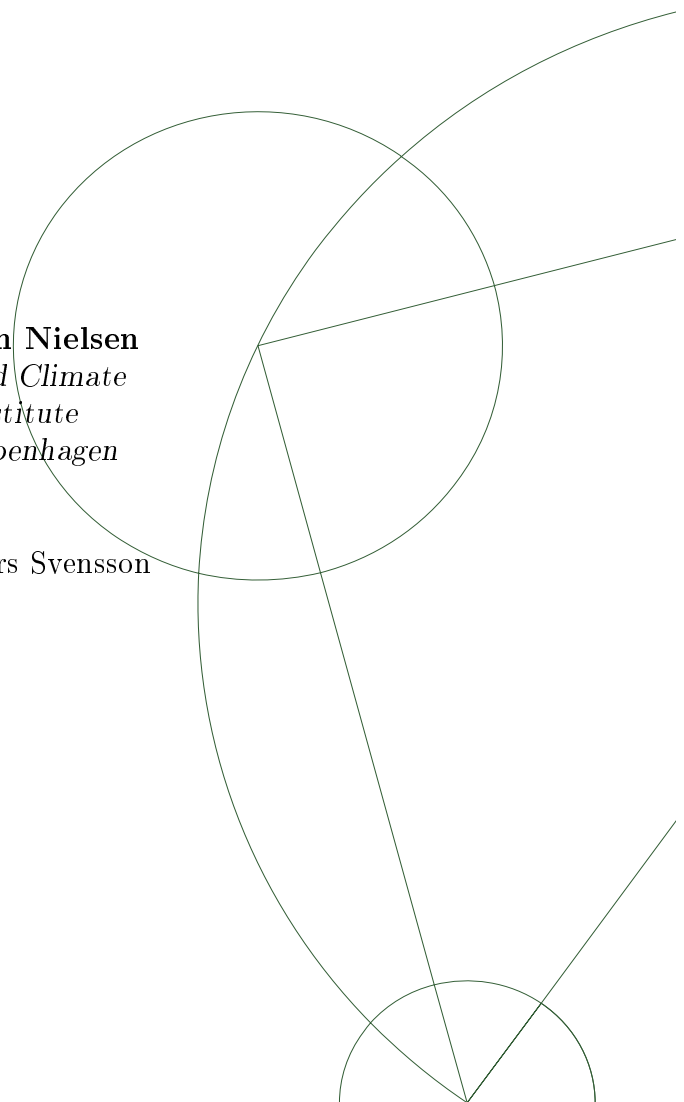


Master thesis in geophysics August 13, 2009

Early Holocene and Eemian impurity profiles from the NGRIP ice core

Maibritt Esbjørn Nielsen
*Centre for Ice and Climate
Niels Bohr Institute
University of Copenhagen*

Supervisor: Anders Svensson



Abstract

Continuous Flow Analysis (CFA) describes the method of measuring chemical impurities, insoluble dust, and the electrolytical meltwater conductivity in ice cores. The method is used to obtain a high-resolution paleoclimatic archive of season variations. The measurement is done by continuously melting a $0.55m$ longitudinal section of ice with a cross section of $34mm \times 34mm$ and analyzing the resulting meltwater. The different CFA components; ammonium (a biological component), sodium (a marine component), dust (insoluble desert dust), and conductivity (a bulk signal of all ionic constituents) are analyzed by fluorescence spectroscopy, absorbance spectroscopy, by a particle detector and with a conductivity meter respectively.

CFA profiles are obtained from four sections of the North Greenland Ice Sheet Project (NGRIP) ice core; Holocene section ($1378.30m - 1389.30m$), an Early glacial section from Dansgaard-Oeschger Interstadial 25 ($2995.30m - 2997.50m$), a section from the transition between the Eemian interglacial and the glacial ($3039.85m - 3042.05m$), and finally a section from the Eemian period ($3069.00m - 3071.20m$).

Dust levels are seen to be subject to a mean concentration difference compared to earlier obtained results and sodium experiences negative and drifting baseline values presumably due to pressure problems in the setup. Therefore improvements in general of the setup are suggested, especially with regard to improving the sodium signal but also towards the construction of the debubbler.

The mean level concentrations of the four components show non-linear dependency with the $\delta^{18}O$ temperature proxy and suggest a saturation level on the basis of the mean concentration levels of the 5 degree warmer Eemian period compared to the Holocene.

A dating of the profiles match well with other time scales for the Holocene section, but a dating of the Eemian section shows a difference in mean annual layer thickness of $0.35 \frac{cm}{year}$ compared to the ss09sea model which correspond to 328 extra Eemian years in the bottom $16m$ of the NGRIP ice core.

Acknowledgement

Thanks to the people who have supported me during my study. First and foremost my supervisor, Anders Svensson for advising; Ernesto Kettner for good discussions in the lab; Matthias Bigler for co-supervising; Centre for Ice and Climate and the employees for providing ideal writing conditions and professional support; Christian Riis for proofreading; Susanne Buchardt for proofreading; and last but not least, my office buddies for fun, laughs and good discussions.

Preface

This thesis covers the final exam of the master degree in geophysics at the University of Copenhagen. It accounts for approximately a year of full time study and hence 60 ECTS points.

A basic knowledge of physics and mathematics is required to read the thesis along with some introductory knowledge of geophysics including especially glaciology. Specific terms and abbreviations within this study are shortly explained. Matlab has been used for the data processing. Time scales are shown opposite of normal — backwards along the abscissa — since this is the common and logical use in studies of past time periods.

ECTS-point	60
Supervisor	Anders Svensson
Co-Supervisor	Matthias Bigler
Name of department	Centre for Ice and Climate Niels Bohr Institute University of Copenhagen
Author	<hr/> Maibritt Esbjørn Nielsen
Date	August 13, 2009

Contents

1	Introduction	1
1.1	Continuous Flow Analysis	4
2	Ice core analysis	6
2.1	Seasonal variations and climate records	6
2.2	Sources and transport routes	12
2.3	Other measurements in ice core analysis	18
3	Samples	22
4	Setup	24
4.1	Description of the instruments used	24
4.2	Resolution	32
4.3	Data processing	37
5	Results and discussion	41
5.1	The Holocene profile	41
5.2	The Eemian and Early glacial profiles	48
6	General discussion	54
6.1	Eemian annual layers and ss09sea	54
6.2	The atmospheric aerosol load through time	55
6.3	Mean levels of impurities - Eemian versus Holocene	59
6.4	Resolution of NGRIP compared to GRIP records	60
6.5	Neutralization of the ice	61
6.6	Improvements of the setup	64
7	Conclusion	67
8	Danish summary — Dansk resumé	69
A	Greenland interstadials	70
B	Additional results	71
	List of figures	73
	List of tables	74
	References	75

1 Introduction

One of the most evolving discussion topics today is the climate. What will our future climate be like, and are we able to predict this by studying the past climate? The effect of human impact on the climate is the main part of the discussion these days, and this impact is exactly the interest of the Intergovernmental Panel on Climate Change (IPCC). Their job is to evaluate the risk of climate change caused by human activity. The latest report is the Fourth Assessment Report which predicts a global temperature rise of a couple of degrees before the year 2100 [IPCC, 2007]. This risk has to be taken seriously, and therefore thousands of scientists around the world are right now figuring out ways to stop or decrease this global warming. In order to decrease the warming, we have to understand the past so that we know what the sources of climate change are.

This is exactly why studying ice cores is of such great interest. This very pure, cold, hard ice hides a great deal of information about the past climate. So where and how do we obtain this ice? On the ice covered island of Greenland several deep drillings of ice cores have been made during the last several decades. The first ice core from Greenland was the Camp Century ice core drilled by the Americans, and it was the first ice core project to drill all the way through the inland ice. The drilling ended in 1966. After this, other cores were drilled. In Figure 1 the drill sites on Greenland are shown, and at this moment a new ice core drilling in Greenland has started. This is the North Greenland Eemian Ice Drilling (NEEM). The ice core from this drilling hopefully carries completely new information. The drilling is supposed to reach bedrock in 2010/2011 and contains ice from the last interglacial, the *Eemian*, period. In Figure 2 the $\delta^{18}\text{O}$ (see section 2.1) record from the NGRIP core is shown on a depth scale (top) and on an age scale (bottom). $\delta^{18}\text{O}$ is a temperature proxy used in ice core research. The figure gives an overview of the present interglacial, the *Holocene*, the last glacial period, and the previous interglacial, the Eemian period. The transition from glacial to interglacial, which included first a small warming period called *Bølling-Allerød* and next a small cold period called *Younger Dryas*, is shown.

For my study I am using ice from the North Greenland Ice Sheet Project (NGRIP) core as the NEEM ice drilling has not yet finished. The NGRIP core, which also contains ice from the last interglacial, is unfortunately affected by bottom melting. This means that the ice near bedrock is at the pressure melting point -2.4°C , and this will affect the annual layer thickness towards the bottom. The deepest layers will be thicker than with no bottom

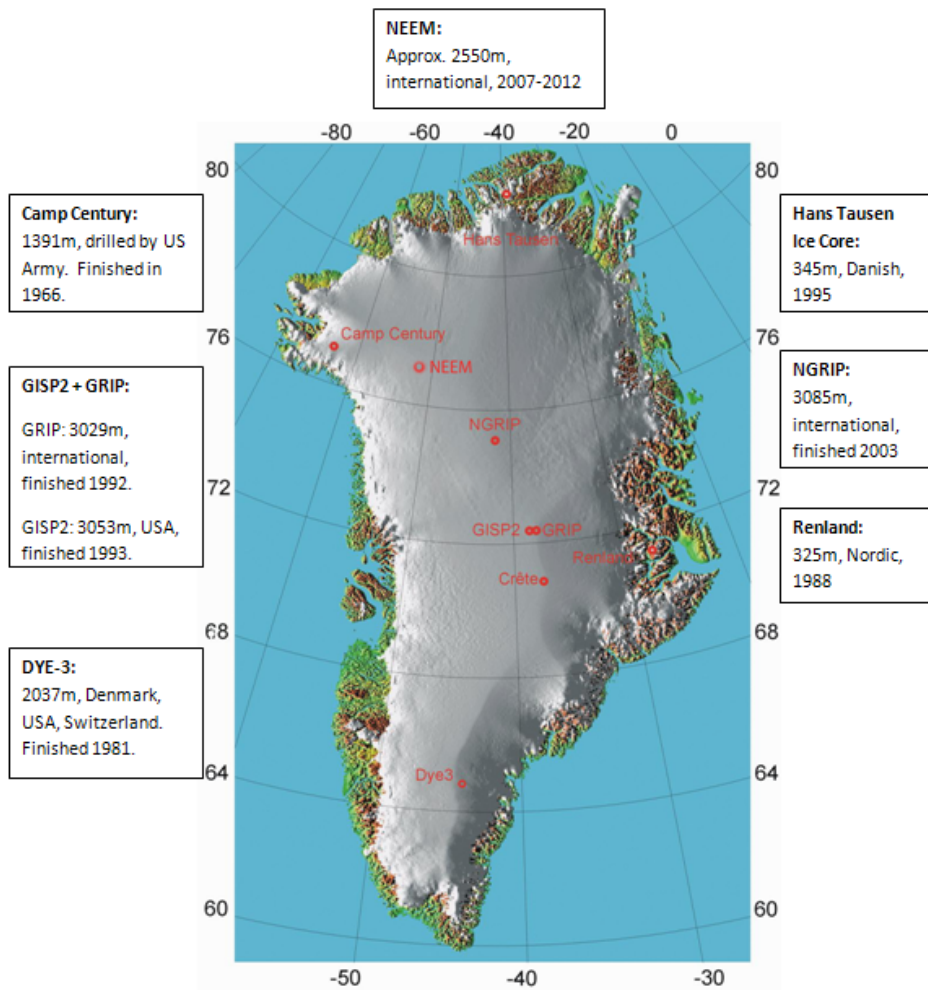


Figure 1: A map of Greenland with location of drill sites. NGRIP is located at 75.12°N 42.32°W. Drilling facts are from [Centre for Ice and Climate, 2009].

melting. The NEEM ice core drilling is geographically located on the basis of minimizing bottom melting.

This thesis will try to show that we are able to observe interesting information about the climate all the way back to the Eemian period despite the bottom melting. Ice from the Eemian period is located in the very bottom of the Greenland ice sheet at the NGRIP site.

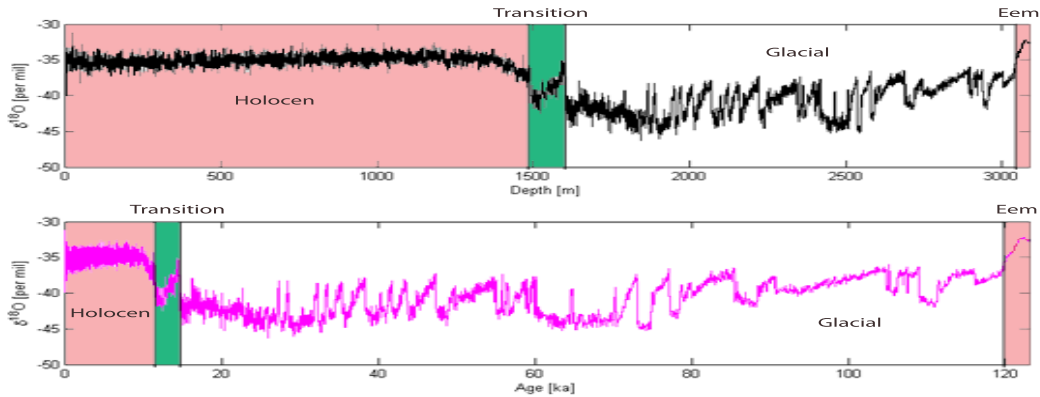


Figure 2: Record of the $\delta^{18}\text{O}$ climate proxy. Top panel shows $\delta^{18}\text{O}$ on a depth scale, and the bottom panel shows $\delta^{18}\text{O}$ on an age scale. The warm periods, Holocene and Eem, are indicated with a light red color, and the transition from the last glacial period to the Holocene period is indicated with a green color. The transition included the warm period, Bølling-Allerød, and the cold period, Younger Dryas.

So what *is* hiding in the ice cores that make them so interesting to study? “Impurities” is the answer. The main purpose of impurity analysis is to obtain information on changes in atmospheric transportation and chemistry, to discover the sources and sinks of the impurities, and to analyse what depositional effects exist. This is all resolved from an impurity analysis, and with a high temporal resolution, information on changes of the atmospheric aerosol load over the last several hundred thousands of years can be obtained.

The method to obtain detailed records of impurities is called Continuous Flow Analysis (CFA) which I will describe in further detail at the end of this section. I have used a completely new CFA setup, located in Copenhagen, for my thesis results. This setup, the *CIC¹ setup*, is in part a copy of the setup used at University of Bern, *KUP² setup* (described in Kaufmann et al. [Kaufmann, 2008]), but the CIC setup does not measure as many components as the KUP setup which means that our temporal resolution can be much higher because a smaller amount of sample water is required.

Why do we want a higher temporal resolution? The important result, when measuring impurities, is that these impurities often exhibit seasonal

¹Centre for Ice and Climate.

²Klima- und Umweltphysik

variations which means that we are able to identify the annual layers in the ice where they still exist. The annual layering of impurities are sometimes affected by for instance bottom melting, diffusivity processes, and bottom topography which can result in a disturbance of the ice. If the time resolution is high enough, centimeter thin annual layers can be observed and according to the ss09sea, which is a modelling of annual layer thicknesses [Johnsen, 2001], the annual layer thickness of the Eemian ice in the NGRIP ice core is approximately 1.47cm. Measuring chemical impurities in the Eemian ice has not been done on Greenlandic ice cores before this study but will also be done with the NEEM ice core drilling. Identifying annual layers are important in the dating of ice cores.

Another purpose with this thesis, besides detecting annual layers, is to study the concentration levels of the impurities. These levels will hopefully tell us something about the past climate which can be compared to the present climate and perhaps give us an idea of the future climate. The last interglacial was about 5 degrees warmer than the Holocene in Greenland, and with the IPCC predicted temperature rise then the future climate might resemble this.

1.1 Continuous Flow Analysis

A continuous flow analysis is done by placing a longitudinal section of an ice core on top of a melting device located inside a freezer. The ice is then melted continuously while the inner and outer part of the ice section is separated in order to avoid contamination. It is important only to remove what is necessary of the outer parts in order to have enough sample water to do measurements on. This sample water contains impurities and air bubbles captured in the ice, and although the air bubbles carry a lot of information about the gases in the past atmosphere they are a waste part in our setup right now. With the CIC setup, four components are measured. These are ammonium, NH_4^+ , sodium, Na^+ , insoluble dust, and the electrolytical meltwater conductivity (from here on *conductivity*). If more components are added to the setup, the temporal resolution will decrease. A picture of the CFA setup in Copenhagen, where the freezer with the ice section is located left of the picture, is shown in Figure 3.

After measuring the ice section, a processing of the data is done. A calibration of each component, except conductivity, is required, and artifacts in the ice core or problems during the runs have to be removed. When this is all done, the results are ready to be analyzed. Ice from the Holocene period and the Early glacial and Eemian period is measured. These sections are then

used for dating purposes where the Holocene CFA profiles will be compared to the GICC05 time scale (described in section 2.1), and the Eemian–Early glacial CFA profiles will be compared to the ss09sea model (also described in section 2.1). For part of this, a fourier transform, which can identify the annual layer peak and give an estimate of the resolution of the setup, will be used. A comparison, especially with regard to concentration levels of the two sections, Holocene and Eemian–Early glacial, will also be presented. When analyzing the results, comparisons with other data will be used as well.

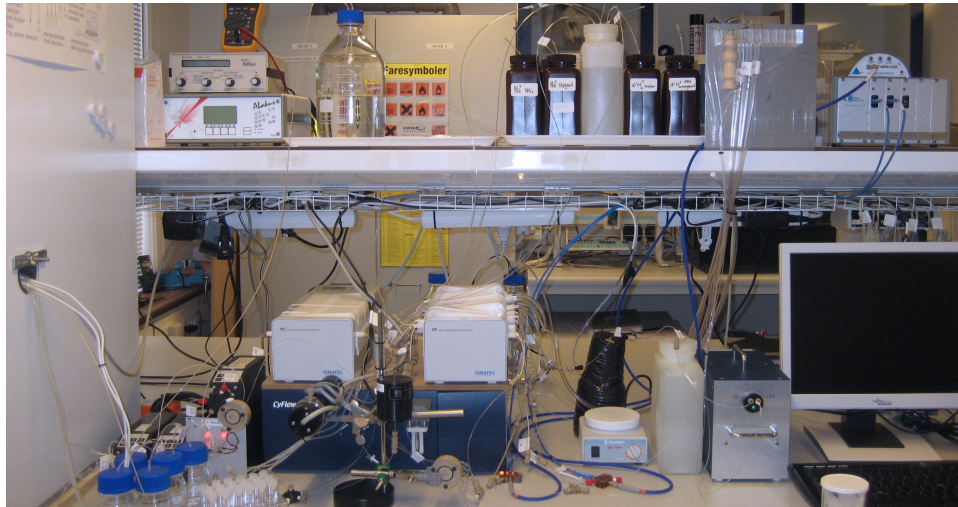


Figure 3: A picture of the setup. The freezer is located left of the picture, the standards in the bottom left, the peristaltic pumps and analysis instruments in the middle, and the computer in the right side of the picture.

Outline

Section 2: In section 2, I will go through the basic knowledge of ice core analysis required for my study.

Section 3: In section 3, I will describe from where my ice samples are taken.

Section 4: In section 4, I will describe the CIC CFA setup in further detail including a look into the resolution of the setup.

Section 5: In section 5, I will present my results obtained with the CIC CFA setup.

Section 6: In section 6, I will give a discussion of my results and comparisons with other data.

Section 7: In section 7, I will presents my conclusions of the study.

2 Ice core analysis

2.1 Seasonal variations and climate records

When snow falls year after year on top of the Greenland ice sheet, the layers are gradually compressed by the weight of the overlying layers, and this produces annual layers down through the ice sheet. As the snow is transformed into ice and moves downward and to the sides, the annual layer thickness decreases so at the bottom, a high resolution analysis is required to observe annual layers. See Figure 4. A chronological order of annual layers down through the ice cap is produced as seen in Figure 5. If bottom melting occurs, the annual layers will not be as thin, but the oldest ones will melt away.

When we analyse ice cores from Greenland, we observe seasonal variation in different parameters for instance in the $\delta^{18}\text{O}$ climate proxy value but also in the chemical impurities. These parameters can be used for counting the annual layers and hence give a quite accurate dating of the ice core.

Stable isotope method

When dating the ice cores, different parameters and methods are used. The $\delta^{18}\text{O}$ value is a corner stone in dating processes of ice cores.

The ocean water consists mainly of $H_2^{16}\text{O}$ but also isotopes, $H_2^{17}\text{O}$ and $H_2^{18}\text{O}$ are present. Due to small differences in the vapour pressure of the different water isotopes, the heavier isotope $H_2^{18}\text{O}$ will have a slightly harder time evaporating than the lighter isotope $H_2^{16}\text{O}$, as well as the heavier isotope will condense slightly easier than the lighter isotope. This will therefore

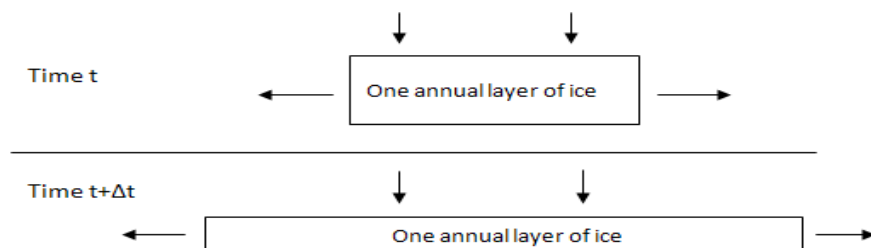


Figure 4: A sketch of a box of ice moving downwards through the ice sheet. At time, t , the box has certain dimensions, and at time, $t + \Delta t$, the box has been flattened and elongated due to the weight of the overlying layers.

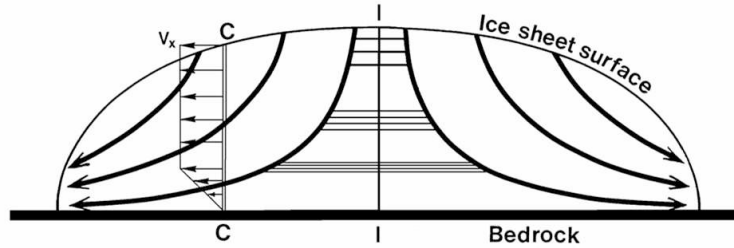


Figure 5: A sketch of the movement of ice in an ice sheet. Flow lines are indicated and goes down and outwards towards the edges. I indicates the ice divide where a chronological order of annual layers can be obtained, and when standing at C , v_x indicates the horizontal velocity of the ice flow.

result in a difference in the fraction of the ^{18}O isotope concentration to the ^{16}O isotope concentration in evaporation and precipitation processes. This means that when an air mass cools and condenses to form precipitation, the remaining water vapour will be increasingly depleted in the ^{18}O isotope. As the amount of precipitation from an air mass, since its last water uptake, depends on the temperature gradient from source area to the place of deposition, and that the temperature over ice varies much more than over sea, the fractionation of the two isotopes will depend on the temperature over the ice. The fraction between the concentration of ^{18}O and ^{16}O is given by the $\delta^{18}\text{O}$ value in an ice sample:

$$\delta^{18}\text{O} = \left(\frac{\frac{[^{18}\text{O}]}{[^{16}\text{O}]}_{\text{sample}} - \frac{[^{18}\text{O}]}{[^{16}\text{O}]}_{\text{VSMOW}}}{\frac{[^{18}\text{O}]}{[^{16}\text{O}]}_{\text{VSMOW}}} \right) \cdot 1000 \text{ ‰} \quad (1)$$

where VSMOW is the Vienna Standard Mean Ocean Water which has a known isotopic composition. Due to the definition, and that glacier ice contains less ^{18}O than VSMOW, the $\delta^{18}\text{O}$ value is always negative. The more negative, the colder the climate is.

As the $\delta^{18}\text{O}$ value is higher, i.e. less negative, during the summer than during the winter, it is possible to identify the annual layers from for instance the summer peaks. It will only be possible, though, to detect these annual layers down to a certain depth because they get too thinned out which makes it difficult to distinguish the winter signal from the summer signal. The $\delta^{18}\text{O}$ value is related to temperature [Dansgaard et al. 1969] and therefore gives a

good picture of the climate back in time even though it will not resolve the annual layers.

Different methods are used for measuring $\delta^{18}\text{O}$. One method is using a mass spectrometer which deflects the molecules more or less depending on the mass of the molecule. Another measurement is using a laser spectrophotometer where the absorbance of the laser light is measured. This absorbance depends on the properties of the molecules.

An overview of impurities measured in ice cores

Besides the $\delta^{18}\text{O}$ value, other climate parameters are measured in ice cores. Air bubbles trapped in the ice allow analyses of atmospheric concentrations of trace gases. Besides gases, dust can be trapped in the ice. Large amounts of dust can come from volcanoes in form of ash. Some volcanic ash layers are so pronounced that they can be seen in ice cores all over the world. These layers serve as reference layers and can be used in the important synchronization of ice core records. Analyses of impurities such as ammonium, sodium, nitrate, and sulphate give information of source areas and transport routes of the atmospheric circulation in the past.

All in all we get proxies for, among others, temperature, precipitation, and we get the chemistry and gas composition of the lower atmosphere, and we will be able to identify volcanic eruptions and forest fires.

When choosing the components that was to be measured with the CIC CFA setup, it was important to have one typical marine component, a typical dust component, and a biological component. The marine component was sodium which is a fall-winter and winter-spring signal due to intensification of the atmospheric circulation in these seasons. The dust component was insoluble dust. Calcium could have been an alternative for dust, but this component is measured by an absorption method which is much more complicated than measuring with an Abakus instrument (see section 4.1). The mineral dust peaks during spring as desert storms are more common at this season. The biological component was ammonium which is mainly an indication of biomass burning events that are more common during summer. Finally a component as conductivity was chosen. This component is also observed with an easy measurement technique which is important for retaining a high resolution of the signal. The conductivity measures a bulk signal of all ionic constituents, both positive and negative. During warm periods the conductivity does not exhibit pronounced seasonal variation as the other chemical components and mineral dust, as it is a measure of the different chemical impurities in the ice that peaks at different seasons. In

cold periods, like the glacial, though, the different impurities tend to peak at the same time, and therefore will conductivity also have an annual peak [Rasmussen, 2006].

CFA profiles

Chemical impurity data is gathered in CFA profiles. The KUP system has been used to measure the NGRIP core, but until now, no Eemian ice has been measured³. The Eemian ice requires a very high temporal resolution, since the annual layer thickness in this depth is around 1.47cm according to the ss09sea model which will be described in the end of this section.

Previous results are important when dealing with a new setup since these can be used to check my results from the CIC setup. If my data compares well with earlier results, it gives me an idea of whether I can trust what I measure in the ice from the Eemian period. As this period has not been measured with CFA before, we do not know what to expect regarding annual layer thicknesses, and whether the impurities in question still exhibit good seasonal variation.

In Figure 6 the results of ammonium, sodium, insoluble dust and conductivity from the KUP setup are shown. The KUP profiles are shown in 5mm resolution and contain data from approximately 1404m to 2930m depth (data is provisional and unpublished). The 5mm resolution means that it will not resolve annual layers from the deep ice very well.

The ammonium record is seen to be especially good when counting annuals. This component has been used for dating in the GICC05 time scale (described in the end of this section) with support of other components. When counting annuals, a fully trustable year counts as 1, and an uncertain year is counted as $\frac{1}{2} \pm \frac{1}{2}$. In the end, the years and uncertainties are summed up [Andersen, 2006]. Figure 7 shows an example of the seasonal variation of the different components during 1m of Holocene ice. Peaks in ammonium are marked with grey vertical bars. It is seen that sodium peaks are in between the ammonium peaks, and dust peaks are right before (on a time scale) ammonium peaks indicating a spring signal.

³From approximately 1404m to 2930m one CFA setup was used, but this setup went missing during a shipment from Antarctica, and a new is therefore built in Bern. This setup has measured impurities from 1394m to 1403m [Kaufmann, 2008].

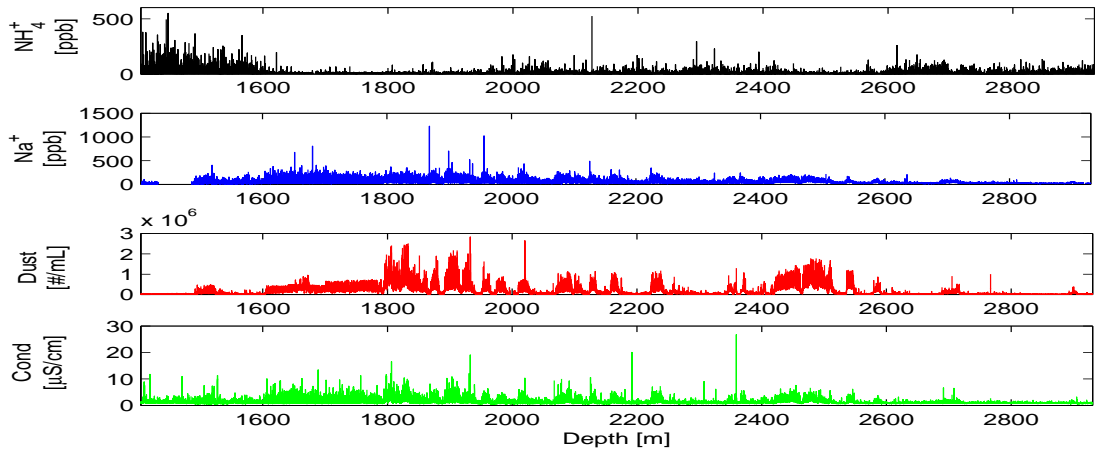


Figure 6: NGRIP CFA profile from depths 1404m to 2930m measured on the KUP CFA setup. Climate variations in the four components are seen as for instance very high dust and sodium values and low ammonium values during the glacial. Data is provisional and unpublished.

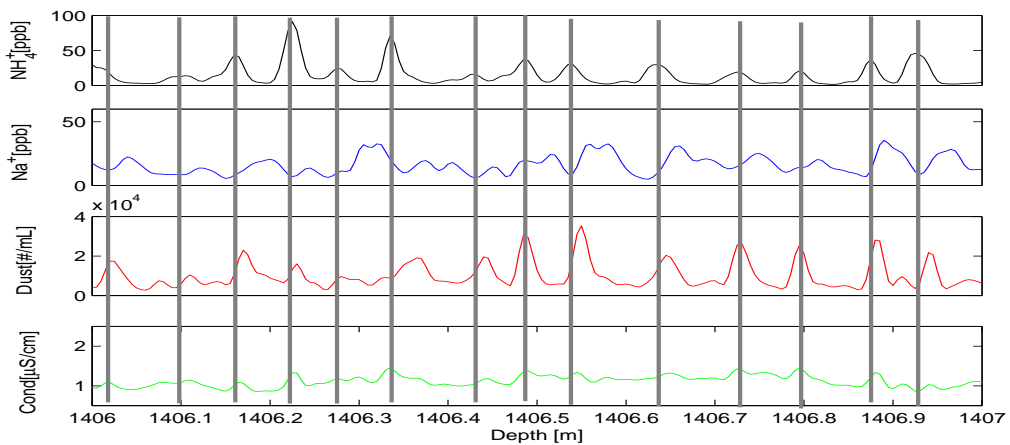


Figure 7: 1 meter of NGRIP CFA profile from depth 1405m to 1406m. Data is provisional and unpublished. Grey vertical bars indicate peaks in ammonium. The seasonality of the other components is seen. Sodium peaks are in between the grey bars, and dust is mainly right before, indicating a spring signal.

Time scales used in ice core research

Time scales are important in ice core research because dating the Greenland ice cores will provide a paleoclimatic archive in which the absolute dating can be performed continuously by counting annual layers from present day and into the glacial period. Different countings of Greenlandic ice cores are matched together into the Greenland Ice Core Chronology 2005 (GICC05) which dates the cores back to approximately $60ka$ b2k⁴ [Svensson, 2008] with a maximum counting error of approximately 4% in warm interstadials to 7% in cold stadials [Andersen, 2006]. When annual layer counting is not possible, modelling of the climate can be used as for instance with the ss09sea model. Below is a short description of the GICC05 and ss09sea time scales.

- **GICC05:** In 2005 a multiparameter counting of annual layers was developed for the last $42ka$ and later extended to $60ka$. The time scale is based on different types of measurement on ice cores from DYE-3, GRIP and NGRIP. It is important to have several independent datings of the ice cores to avoid the risk of missing annual layers. Comparisons with other time scales are made, for instance with the ss09sea model. The two time scales generally compares well, but the GICC05 suggests that the model underestimates the duration of certain intervals, but also that this is compensated for in other parts of the model. Figure 8 gives an overview of which analysis techniques that have been used at which depths when constructing the time scale.

- **ss09sea:** ss09sea is a modelled time scale. It was initially constructed for the GRIP ice core and was later applied to the NGRIP ice core. This time scale is constrained by two fixed points; the Younger Dryas/Holocene transition at $11.554yr$ b2k and the transition at $110ka$ b2k occurring in GS-25⁵. ss09sea is a modelling of the thinning of annual layers with the use of an accumulation model based on sea-corrected measured $\delta^{18}O$ values. The GICC05 and ss09sea time scales show good agreement overall although the ss09sea from Last Glacial Maximum (LGM) and back to $42ka$ b2k shows thinner annual layers than GICC05. This indicates that the model tuning parameters may need some adjustments [Svensson, 2006]. Figure 9 shows a comparison of the two time scales back to $42ka$ b2k. Figure 10 shows the full profile of annual layer thicknesses modelled down to the bottom of the

⁴before the year 2000

⁵GS-25 is a cold period during the last glacial. See Appendix A

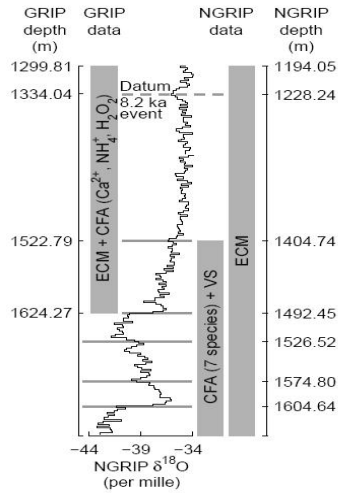


Figure 8: An overview of the data series used for the different parts of the GRIP and NGRIP ice cores in order to construct the GICC05 time scale. VS=Visual Stratigraphy, ECM=Electrical Conductivity Method. [Rasmussen, 2006] – modified.

NGRIP ice core. Figure 10 also shows the $\delta^{18}\text{O}$ values and a section of $\delta^{18}\text{O}$ and annual layer thickness values from the Eemian and Early glacial.

2.2 Sources and transport routes

An overview of the sources, variations, and correlations of the chemical impurities, dust and conductivity in and of the ice cores, that are of interest for this thesis, are given in this section.

Ammonium

Ammonium, NH_4^+ , originates from biomass burning, anthropogenic emissions as for instance excreta and fertilizer losses, and soil and vegetation. The variations depend on changes in transport routes, deposition mechanisms, and furthermore changes in the source regions and source strengths [Fuhrer, 1996]. Ammonia, NH_3 , is emitted into the atmosphere for instance during biomass burning events. It is responsible for part of the neutralization of the atmospheric acidity. Ammonium salts (mainly sulphates) are the principal component of the submicrometer fraction of atmospheric aerosols, and ammonium is therefore responsible for a degradation of atmospheric

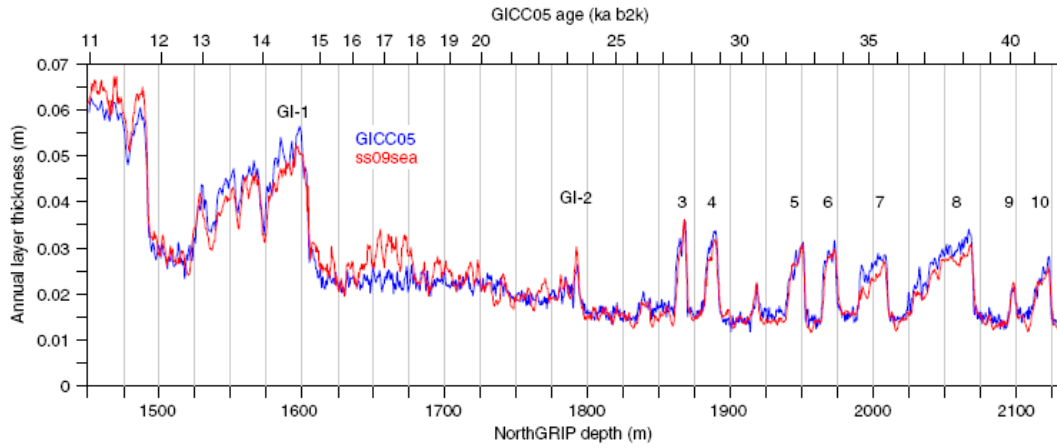


Figure 9: Comparison of annual layer thicknesses between the ss09sea and GICC05 time scales. The two time scales show overall good agreement despite thinner ss09sea annual layers from LGM and back to 42ka. [Svensson, 2006]

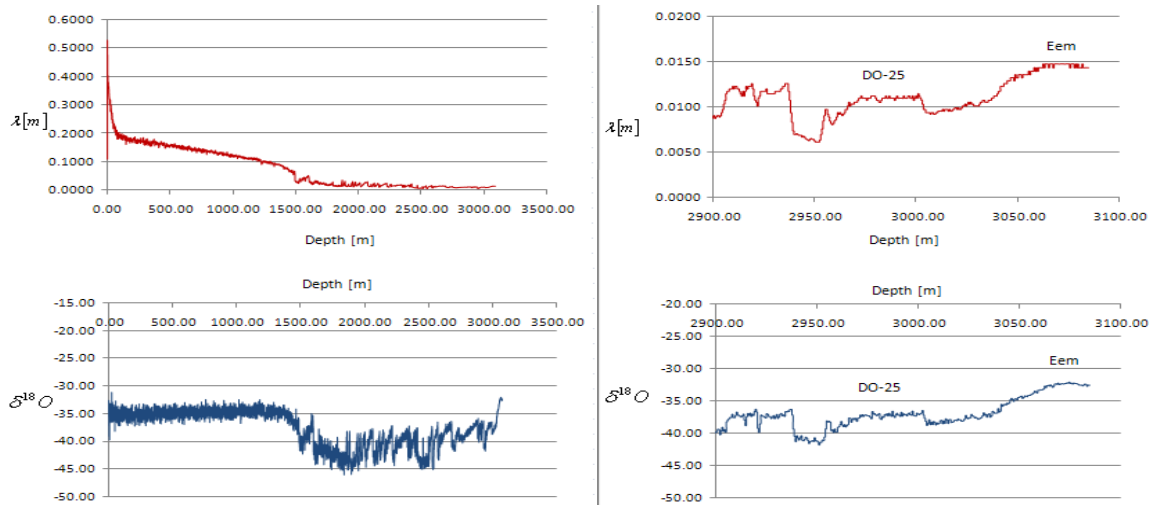


Figure 10: Left panel shows the full profile of ss09sea annual layer thicknesses, λ , in meters together with the $\delta^{18}\text{O}$ values. Right panel shows a segment of the model containing my Eemian and Early glacial periods. The Eemian period and Dansgaard-Oeschger event DO-25 are indicated.

visibility [Genfa, 1989].

The ammonia molecule acts as a weak base and reacts in the atmosphere to form ammonium sulphates. The ammonium ion is then recorded in the analysis of ice cores. There has been recorded no overall anthropogenic increase in ammonium over the last 300 years, but the spring concentrations has doubled since 1950 which could indicate the effect of industrialization [Fuhrer, 1996]. Before the industrialization, biomass burning events were a major source of ammonium in ice cores. This source accounts for about 10 to 40 percent of the ammonium concentration found in Greenland ice cores during the Holocene [Fuhrer, 1996]. There has been recorded no correlation between the area burned in North America and the summer concentrations over the last 100 years. North America is considered the main source area of the ammonium concentration found in Greenland ice cores due to the western atmospheric circulation pattern.

The ammonium, which comes from natural sources such as vegetation and soils, is seen as a background signal in the ice cores. The ammonium record shows very low values during the winter. The background signal has also been decreasing during the Holocene. This suggests that the temperatures has gone down because such a trend will cause a lower ammonia emission. Variations in flux (concentration times accumulation) gives a hint of in which directions possible changes in form of deposition and transport routes in atmospheric circulation occur.

Sodium

Sodium in ice cores derives mainly from sea-salt. Sea-salt as an atmospheric aerosol load has an active role in the Earth's climate system. It can be used to reconstruct the climate conditions in the source regions as well as the large-scale atmospheric transport patterns. The sea-salt load depends on cyclonic activity and wind speeds. High wind speeds produce an efficient sea-salt aerosol formation as well as efficient transportation [Fischer, 2007].

Sea-salt is deposited both by dry and wet deposition. The amount of sodium from wet deposition is proportional to the snow accumulation, but the amount of sodium from dry deposition is not calculated as straight forwardly. The sea-salt derives both from open ocean dispersion and from sea-ice, and the influence of one derivation compared to another is still an open question. The dispersion of seawater over the open ocean depends on the wind speed. The amount of sea-salt therefore depends on cyclonic activity especially along polar fronts in both hemispheres. We still need more studies on the sea-salt sources to answer the question of how much influence

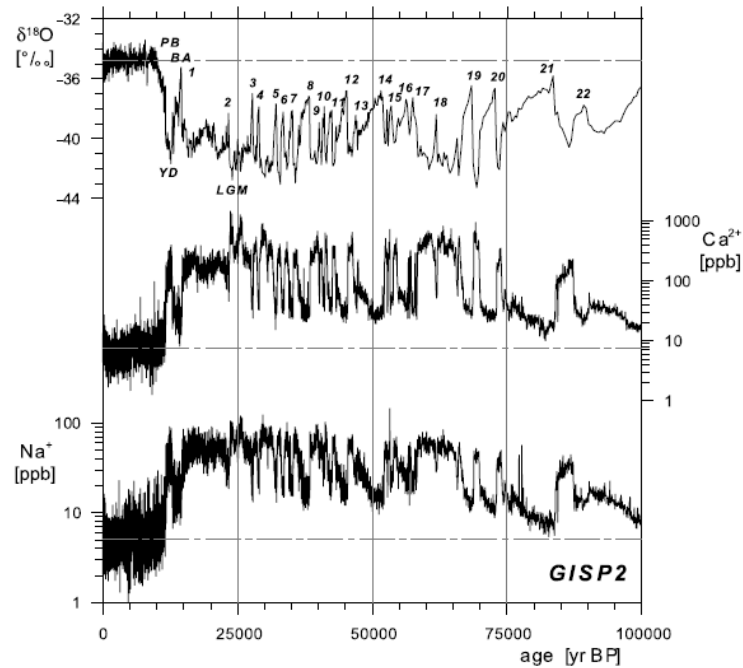


Figure 11: The chemical dust component Ca^{2+} , and the sea-salt component Na^+ over the last glacial cycle as recorded in the GISP 2 ice core. Also marked are the Preboreal (PB) period and the Last Glacial Maximum (LGM) as well as rapid climate events such as the Younger Dryas (YD), the Bølling/Allerød Oscillation (BA), and the Dansgaard-Oeschger events 1-22. Dashed-dotted lines indicate Holocene levels ([Fischer, 2007] Figure 2).

the sea-salt emission from sea-ice has [Fischer, 2007].

During the glacial periods the load of sea-salt as well as mineral dust and calcium is much larger than in the interglacial periods (See Figure 11). This is a result of stronger sources, more efficient transport, and/or less deposition en route.

As the sodium component in ice cores mainly derives from sea-salt (NaCl), we have a positive correlation between sodium and chloride since they both have a common marine source. As the ratio between sodium and chloride has been observed to be around the same ratio for these components in sea-water, we can conclude that the main source must be sea-sprays [Busenberg, 1979].

Higher values may be due to crustal addition from coastal Greenland and dust from Asia in winter. The sodium concentration usually has fall-winter and winter-spring highs caused by the intensification of atmospheric circulation during these seasons. Occasional summer highs in the sodium concentration could be explained by melting of sea ice during summer which increases the open ocean areas.

A study of the sodium/chloride ratio of old preindustrial ice and new ice shows that the geochemical cycle of Na^+ and Cl^- has not been affected very much by industrialization. The old ice had a ratio of 2.2 and the new a ratio of 2.1, compared to seawater with a ratio of 1.8 (chloride to sodium) [Busenberg, 1979].

Mineral dust

Dust (windblown mineral aerosols) is the most abundant primary aerosol in the atmosphere apart from sea-salt. It enhances marine bioproductivity [Ruth, 2008], and to understand the past climate, it is necessary to have an accurate quantitative reconstruction of the past atmospheric dust loads and the aeolian⁶ dust fluxes. The dust compound is also important in formation and development of soil in remote land areas. The most common proxy for dust is to measure the insoluble particle concentration but sometimes also the concentration of calcium ions is used. When measuring the dust compound, it is often not specified which proxy is used, and we do not know how they quantitatively relate to each other [Ruth, 2008].

There is usually a very big difference between the dust loads during cold periods and warm periods. When it is cold, it is often very windy and dry. This brings a lot of dust to the ice core sites, and therefore we often see that the different climatic periods differ in dust concentration by a factor of ~ 100 although this factor differs by a factor of 2 depending on the methods used for analyzing [Ruth, 2008]. Dust is a local factor and can hence vary a lot from ice core to ice core whereas the gaseous impurity species are mixed globally and will often be similar from core to core.

The volume distribution of the dust particles also vary between warm and cold periods. According to Ruth et al. [Ruth, 2003], a single lognormal distribution can describe the bulk of the particle volume. The modal diameter or “mode”, μ , describes the dominating diameter of the particles, and it varies systematically with $\delta^{18}O$. During warm periods, like the Preboreal period, $\mu = 1.3\mu m$, and during cold periods, like at LGM, $\mu = 1.7\mu m$ (see

⁶Wind driven.

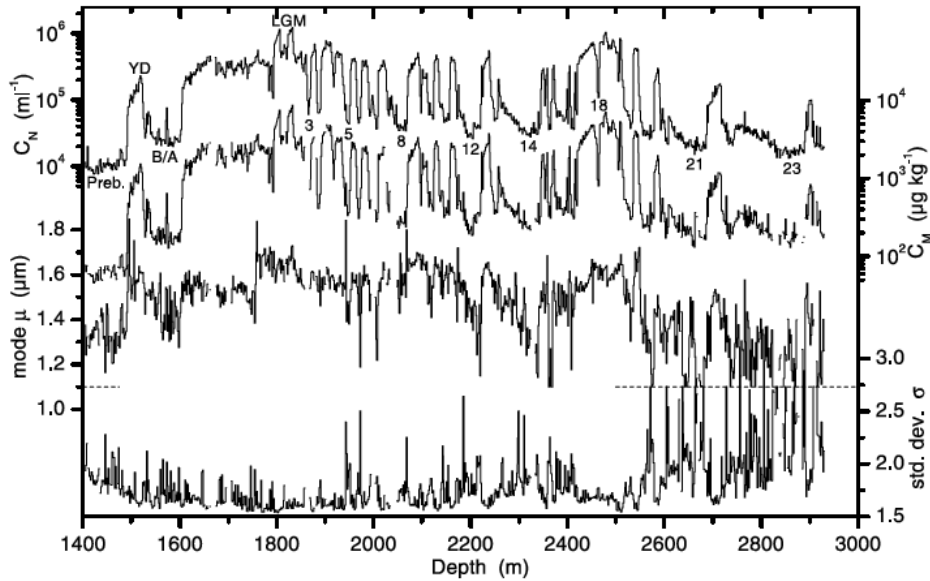


Figure 12: Profiles of microparticle concentration, C_N , and lognormal size distribution parameters, μ (diameter) and σ (standard deviation). C_N is based on particles larger than $1\mu m$ in diameter. Gaps arise from missing data or from data that did not allow for a proper lognormal fit. Preb=Preboreal, YD=Younger Dryas, B/A=Bølling-Allerød, LGM=Last glacial Maximum. Numbers refer to DO events. The data from the bottom two panels was truncated at the dashed line. [Ruth, 2008]

Figure 12); that is during cold periods, the dust particles are a lot coarser than during warm periods due to a difference in the long range atmospheric transport time. Coarser particles will be more common on shorter transport routes because they will not be depleted en route.

Conductivity

Conductivity is a bulk signal of all ionic constituents. Large sulphate peaks — due to volcanic eruptions and non-eruptive volcanoes — often show up in the conductivity signal since the volcanoes emit SO_2 to the atmosphere which then reacts to form H_2SO_4 . As calcium is a soluble dust ion, the conductivity measurement will also detect this ion and will therefore sometimes resemble the dust signal. Besides these ions, a big part of the conductivity signal comes from biogenic activity and organic material.

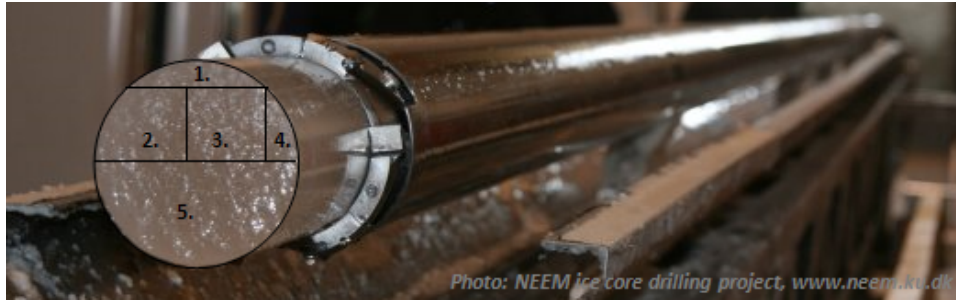


Figure 13: A sketch of the cutting plan for the NGRIP ice core. 1: Physical properties, 2: Gas measurement, 3: CFA, 4: Stable isotope measurement, 5: Shipped to Copenhagen.

2.3 Other measurements in ice core analysis

When an ice core is drilled, it is divided into 5 different sections, and each section is used in a specific analysis. On the NGRIP site, the core was divided into two halves where one half is shipped to a storage freezer in Copenhagen. Figure 13 shows the division of the ice core. Section 1 is used for measuring physical properties of the ice; for instance when mapping the crystal structure. The part consisting of section 2, 3, and 4 is used for Visual Stratigraphy (VS) before separating these sections from each other. Section 2 is used for gas measurements and section 3 is then used for CFA measurements. Finally section 4 is used in stable isotope measurements. Before section 5 is shipped to Copenhagen, it is used for Electrical Conductivity Measurement (ECM). Below I have shortly described three of the analyses, each of which I will use previously obtained results to compare with in my further study.

Gas measurements

By melting or crushing the ice, the past atmospheric air can be released and measured. This air will have a different age than the surrounding ice. When snow falls on an ice sheet it is at first very porous, and as more snow falls on top, it gets more and more compressed. In the top of the ice sheet (approximately down to 80-100 meters) the snow is called firn. The air in this section is not yet closed off from the surrounding atmosphere over the ice sheet. Therefore there can be an exchange of the air in the snow or firn until the so-called *pore close off*. Below this point the air is trapped in the ice and stays there. This process makes the air trapped in the ice younger than the surrounding ice, and this of course has to be taken into account

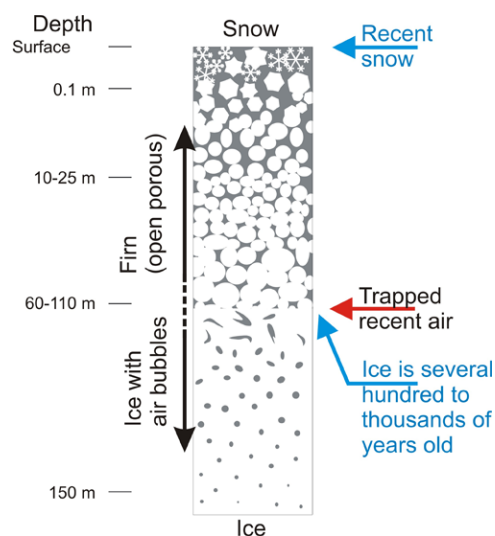


Figure 14: A sketch of the process of snow moving down an ice sheet column while transforming to ice. Air above the *pore close off*, around 80m – 100m, still exchanges with the air above the ice sheet, but below this pore close off, the air is trapped. [Schwander, 1996]

when dating trace gases in the ice. Figure 14 shows the phenomenon. The difference in age is called the Δ age.

The fact that the gases are younger than the surrounding ice can be used when studying the old ice where processes like folding or other disturbance of the layers can occur. If these processes are present, there would be a physical change in the ice which would result in a simultaneously immediate change in the ice *and* the gas. If it is a climate shift, the shift in the gas record will be located further down in the ice than the shift in the ice record; around 7 meters in the Greenland cores [NGRIP members, 2004]. When looking at transitions in the old ice, we have to see the same transition in the gases after a time comparable to the Δ age value, or else this transition could be an indication of ice mixing or folding of the layers caused by bottom topography or disturbing ice flow for instance. Measurements of the NGRIP ice core suggest that this is not the case [NGRIP members, 2004], and therefore we can conclude that no folding has occurred in the Eemian-Early glacial sections I am measuring.

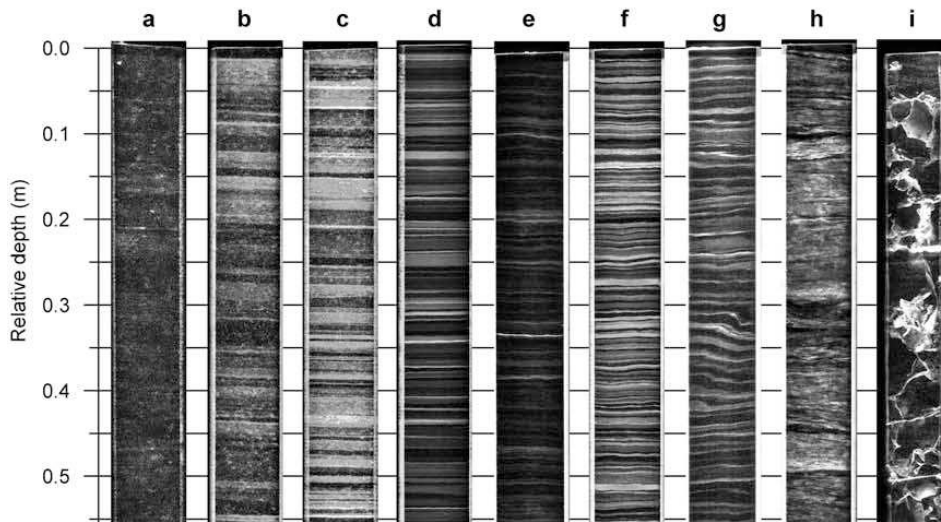


Figure 15: Example of line scan images from various depths. In order to visualize the stratigraphy the contrast of the images is enhanced. (a) Holocene ice, (b) ice from Younger Dryas, (c) cold glacial ice, (d) ice from around LGM, (e) ice from the sharp climatic transition into the mild glacial interstadial 19 (IS19), (f) ice from the cold period preceding IS19, (g) microfolding around 2600m, (h) ice from around 2900m, horizontal layering is blurring out, (i) ice from the Eemian period, visible grain boundaries of large crystals. ([Svensson, 2005] Figure 2)

Visual Stratigraphy

A so-called line scanner is used on a polished section of ice in order to record the visible layering which is especially pronounced in the dirty, glacial ice. I can use these records when choosing which sections of Eemian ice to measure because a picture of breaks in the ice core is obtained, and I would like to avoid such breaks. Towards the bottom, the ice is very warm, nearly at the pressure melting point due to geothermal heat. When the ice is warm, crystals have a tendency to grow larger which will influence the VS profiles of these sections. Figure 15 shows the line scan pictures from different sections of the NGRIP ice core. I have measured ice from just around sections (a) and (i).

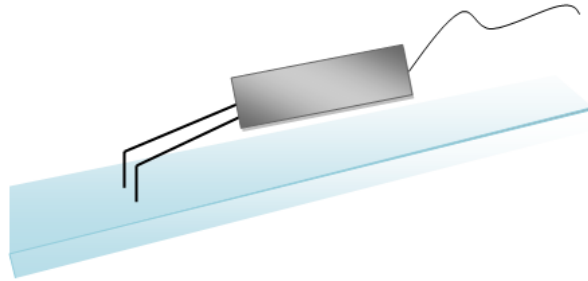


Figure 16: A schematic drawing of the ECM measurement. The two electrodes are simply drawn along the surface and can hence result in small depth differences when comparing the ECM record to other records.

Electrical Conductivity Method

Before section 5 is shipped off to Denmark, it is cleaned with a microtome knife and used for electrical conductivity measurements. A microtome knife is a very sharp knife that peels thin layers of the ice. It is also used for cleaning the surface before linescan measurements. The ECM measurement can be done straight away after the drilling since it only consists of two electrodes drawn along a plain surface of the ice core measuring the conductivity of the ice. The result is a measure of the acidity of the ice since it is mainly H^+ ions that can move freely on the ice surface. The ECM record will reveal past volcanic eruptions because these eruptions emit large amounts of SO_2 , which in the atmosphere is turned into sulphuric acid, H_2SO_4 , that shows up in the ECM record.

Figure 16 shows a schematic drawing of the method used. Unfortunately with this type of method, there can be some uncertainty in the depth scale (pers. comm. Svensson, 2009).

3 Samples

I have measured ice core samples from four depth intervals in the NGRIP ice core. The ice is stored in the freezer at the Rockefeller Institute at -25°C for further investigation. 11m of Holocene ice is measured. I have chosen bags in the interval 2507 to 2526 which correspond to a depth interval from 1378.3m to 1389.3m (Interval 1A). According to the GICC05 time scale this depth section is from the ages 9.920 to 10.060 years b2k., which is just around 1.500 years after the onset of the Preboreal period⁷. This onset is dated to 11.554 b2k [Svensson, 2006].

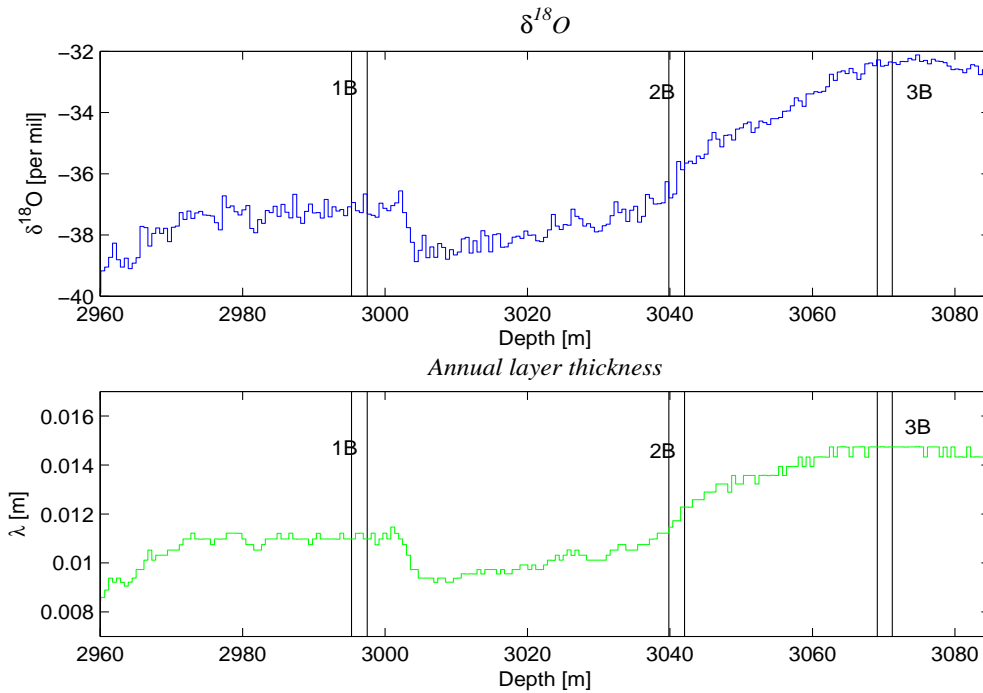


Figure 17: A section of $\delta^{18}\text{O}$ and annual layer thickness (ss09sea). My three Eemian and Early glacial intervals are indicated as 1B, 2B, and 3B.

From the Eemian–Early glacial period I have measured three intervals of 2.2m length each. One section is from the DO-25 event [NGRIP members, 2004] (see Appendix A) and is from the depths 2995.30m – 2997.5m (Interval 1B), one is from around the transition from interglacial to glacial and is from

⁷Preboreal — the period just after Younger Dryas, YD.

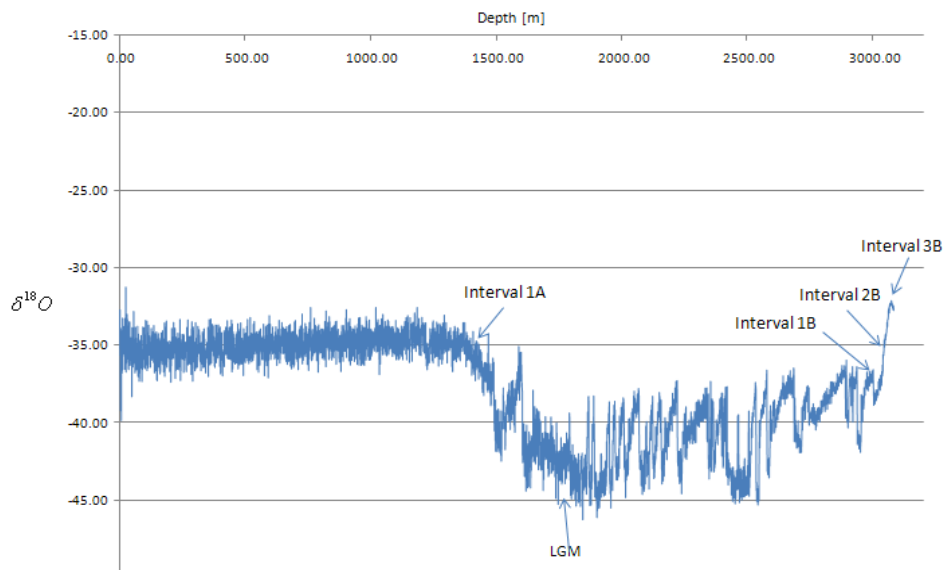


Figure 18: NGRIP $\delta^{18}\text{O}$ record including my sample intervals indicated as 1A, 1B, 2B, and 3B. Last Glacial Maximum is indicated as well.

the depths $3039.85\text{m} - 3042.05\text{m}$ (Interval 2B), and the last one is from the Eemian interglacial, and is from depths $3069.00\text{m} - 3071.20\text{m}$ (Interval 3B). The locations of the three Eemian–Early glacial intervals are marked on the plot of $\delta^{18}\text{O}$ in Figure 17. All four intervals, that I have measured ice from, are indicated on the $\delta^{18}\text{O}$ profile in Figure 18. The samples are chosen with an eye on the line scan images in order to avoid breaks and other artifacts in the ice.

4 Setup

A schematic overview of the CIC setup is shown in Figure 19. The freezer with the ice sample is shown in the left side of the diagram. Below the sample, is a cube of ice made from purified water called mQ⁸ and on top we use one more (not shown on the figure) just under the weight (carriage). The ice is kept in place by the sample holder. Attached to the weight on top is an optical encoder wire.

From the freezer, the ice sample is melted and flows through a tube outside the freezer and is lead through an LED bubble detector. This detector could be used for automatically shifting between ice sample and blank water when there is no more ice, or if the ice gets stuck which will be implemented in the setup at another time. Afterwards the sample is lead through the injection valve. This valve chooses between the ice sample or the blank/standard. From here the sample goes through a debubbler that leads all the gas enclosed in the ice slip out⁹. After the debubbler the sample is checked for bubbles again in another bubble detector. The sample now enters a distributor where it is distributed into four lines. One line goes to the particle detector and another one to the conductivity meter. The sample is sucked through these two instruments since the peristaltic pump is located afterwards. The two other lines go through the pump and are mixed with their respective reagents and buffers before they enter their measuring units. All data is then collected by a computer.

The CIC setup is slightly different from the KUP setup. It has a different melting device, the pump is located after the valves, we have a different melting speed, and the debubbler is constructed in a different way.

4.1 Description of the instruments used

Melting device

The melting device is a unit with an outer dimension of $34mm \times 34mm$. The ice, which is approximately $55cm$ long, is placed vertically on top of the melting device where a melting head is located. The melting head is heated up to about 40 degrees Celsius controlled by a monitor outside of the freezer. The melting head is divided into two sections; an outer one and an inner

⁸“mQ water” or “blank water” consists of purified water. It is cleaned in such a way, that for instance the total organic carbon, TOC, is under 4ppb, and the amount of minerals is low. This is ensured so that the blank water has concentration values of the components, that I measure, close to zero.

⁹This gas could be collected and investigated for atmospheric gas composition.

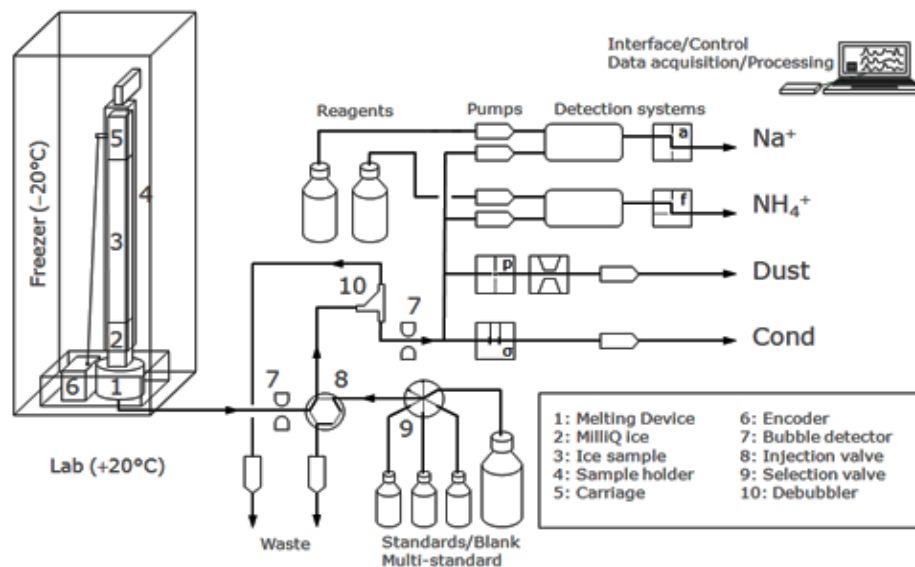


Figure 19: Schematic overview of the setup. The melting device is located in a freezer in the left part of the diagram, and the analysis units are located in the middle and right part. Sketch by M. Bigler - modified.

one. The system sucks the inner section of the melted ice into the sample system via the drain channels, and the outer part is waste (see Figure 20). To ensure that no contamination from the outer parts takes place, a small overflow from the inner part towards the outer part is enabled by pumping a little less water than what the melted ice produces. The dimension of the inner part is $26\text{mm} \times 26\text{mm}$.

The temperature of the melting head is kept constant and together with a small weight on top of the ice it ensures that the melting speed is constant; towards the end where the weight of the ice itself decreases, we usually had to turn the temperature up to keep the desired melting speed. An optical encoder connected to the weight on top of the ice sample keeps track of the melting speed. For my measurements, I want a melting speed of approximately $1.5 \frac{\text{cm}}{\text{min}}$ which produces a higher resolution than earlier measurements with CFA. The problem is to reach the fine line between high resolution achieved by a slow flow rate and enough sample water to inject into the instruments. The latter defines the lower limit for the melting speed.

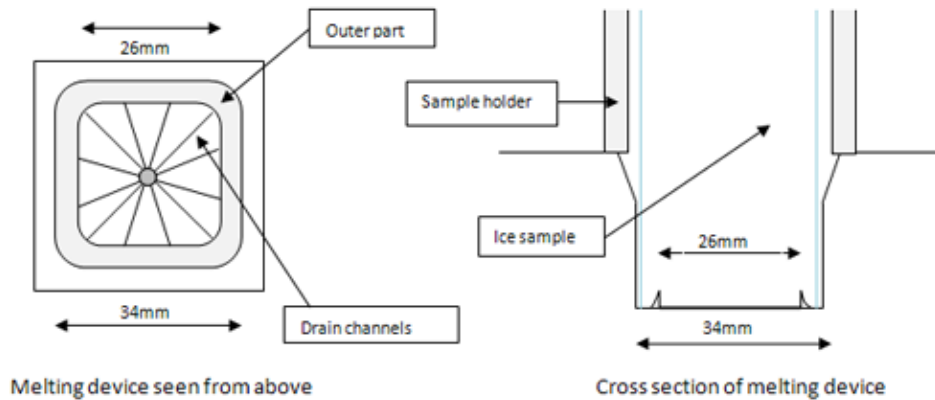


Figure 20: The melting device seen from above and through a cross section. It is seen how the inner and outer parts of the ice core are separated to avoid contamination.

Encoder

The encoder is a wire attached on a weight on top of the ice. When the ice melts, the wire moves down with it, and in the other end of the wire the movement is recorded by an optical encoder. This encoder measures the movement in counts per second and 25 counts correspond to 1mm . With the use of this optical encoder, it is possible to accurately link the measured impurity concentrations to the corresponding depths.

From the differential counts (counts per second), the melting rate can be found and with information on the start depth of the ice segment, the depth scale can be calculated. The start depth can be calculated from the bag number since every bag is 0.55m long when no artifacts are present. Some of the ends of the ice cores are cut off which of course is taken into account. Sometimes there are breaks in the middle of the ice core and to avoid contamination from drilling liquid or anything else, these breaks are cut out and then put back in during the data processing as NaNs¹⁰.

Unfortunately the encoder “jumps” sometimes. It is most likely an error in the software when overload occurs, but it could also be a real jump in the wire. Either way, it ruins data and it needs to be adjusted for in the data processing. This will also have an effect on the accuracy of the depth scale because sometimes the jumps are very small and hence will not be found in

¹⁰Not a Number; which means that no value is assigned.

the processing. In theory the depth scale should be precise down to $\frac{1}{25}mm$.

Fluorescence spectroscopy

The ammonium component is detected using a reagent called o-phthaldialdehyde — OPA. A buffer is added, separately from the reagent, to the sample water in order to improve sensitivity. The chemical reaction is accelerated when the sample water is heated up for which we use a 85°C warm water bath. When this heating happens, the detection sensitivity is further increased. Afterwards the sample is cooled again. This ensures that emerging bubbles, due to the heating in the water bath, are dissolved. Still existing tiny bubbles are afterwards removed with an Accurel which is a small piece of microporous membrane. This piece lets air slip out due to a small overpressure and lets the sample water pass on.

In the fluorimetric detection, the photosensor modules are mounted orthogonally to an LED light source. A mirrored micro flow cell is mounted in the light path for enhancing excitation and emission. In fluorescence spectroscopy a beam of light excites a molecule by absorbance of a photon. The molecule will now be in a new, unstable energy state. The extra energy can be released as heat production by vibrations of the molecule or as radiation because the electron decays to ground state. This will happen by emission of a photon. The emitted light will have a lower energy (or same) and hence a longer wave length than the excitation light. (See Figure 21 for a sketch of the energy levels). Only the emitted light will be recorded. For this an emission filter is used. In my case the intensity of the emitted light will tell me about the concentration of the substance. The higher concentration, the more photons will be emitted and hence a higher intensity is measured.

When calibrating the ammonium signal, I use a standard solution with a concentration of 30ppb. With such low-level standards, extreme care is needed. Freshly deionized water should be used and making sure the standard is not exposed to ambient air is important. Also the standard should be used right away. Especially the ammonium standard can increase in concentration just by standing around. The fluorescence calibration is easy since the concentration acts linearly with respect to intensity. The only adjustment required is to subtract the baseline of the blank (I_{blank}) from the measurement (I). I_{blank} is assumed to be at zero ammonium concentration. Then the concentration is simply calculated from how many counts a given concentration equals, (α_f), as in Equation 2:

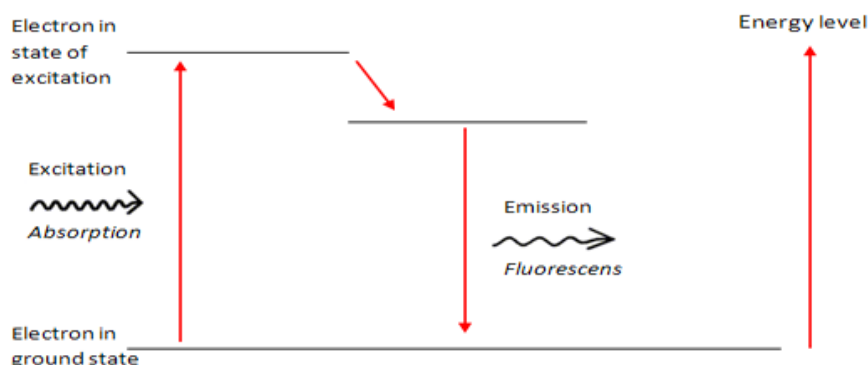


Figure 21: Fluorescence spectroscopy: A molecule is excited into a higher energy state by absorption of a photon, and when the molecule decays to ground state, a photon is emitted.

$$c = \frac{I - I_{blank}}{\alpha_f} \quad (2)$$

A standard calibration is made after every two bags.

Absorption spectroscopy

The sodium component is detected with an absorbance method. The sample water is pumped through the system and at first mixed with a sodium reagent. For mixing, coiled tubings are used. This initializes turbulent instead of laminar flow which then mixes the two individual flows. After this, the sample water is pumped through a reaction column (IMER - IMmobilized Enzyme Reactor). This column consists of a living organism that enhances the sodium signal in the sample such that it is more easily detected.

Afterwards a buffer is added. This buffer increases the pH by adding a $17mM^{11}$ ammonia solution to the flow. The buffer is important for assuring that the pH is nearly constant which keeps the enzyme alive.

The determination of sodium is done by a photometric method which is based on the absorbance of *o*-nitrophenyl that is produced in a hydrolysis of *o*-nitrophenyl- β -D-galactopyranoside (ONPG) catalysed by β -galactosidase [Röthlisberger, 2000]. The enzyme activity then depends on the sodium concentration. Therefore the sodium concentration can be determined by

¹¹milliMolar.

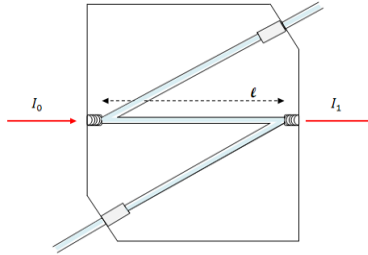


Figure 22: A beam of light illuminates the sample water in order to record the absorption of light, which gives information of the properties of the substance. l is the length of the flow cell, that is illuminated, I_0 is the intensity of the incident light, and I_1 is the intensity of the transmitted light.

monitoring the *o*-nitrophenol concentration. To achieve maximum absorption, we use an ammonia solution of 25% v/v¹² which results in a pH of 9 [Röthlisberger, 2000]. The durability of the IMER is approximately 2 years at 4°C.

Finally the sample is lead through a light path inside a flow cell. The flow cell has a length corresponding to the expected concentrations, usually 10–40mm [Kaufmann, 2008]. The instrument then observes the absorbance of the light through the sample. The measurement depends on temperature, flow rate, and other physical properties.

The absorption of light can empirically be related to the properties of the material the light passes through. This law is called the *Beer-Lambert law*. As my substance flows through a cell and a beam of light shines through the material, a logarithmic dependence, between the transmission, T , and the product of the absorption coefficient, α , of the material and the distance, l , the light travels through the material, is observed.

The absorption coefficient can hence be expressed as a product of the absorptivity, ϵ , of the material and the concentration, c , of the absorbing elements in the material. For liquids we get:

$$T = \frac{I_1}{I_0} = 10^{-\alpha l} = 10^{-\epsilon l c} \quad (3)$$

where I_1 is the intensity of the light after it has passed through the liquid, and I_0 is the intensity of the incident light. See Figure 22. The absorbance

¹² volume to volume

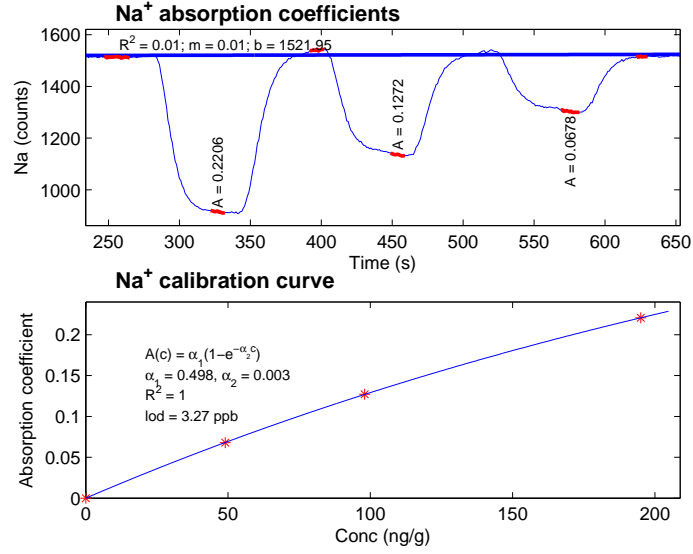


Figure 23: A plot of the calibration method for sodium. Top panel shows the three standard concentrations and the corresponding absorption, A . Bottom panel shows the calibration coefficients calculated from the fit of absorption as a function of concentration.

is for liquids defined as:

$$A = -\log_{10} \left(\frac{I_1}{I_0} \right) \quad (4)$$

When calibrating the signal the trend of the baseline is at first removed. This is defined by the interpolation of the blank level in the beginning and at the end. Next the so-called alpha coefficients are calculated. In Figure 23 the coefficients are found by fitting the exponential relation between absorption and concentration to the standard values. See Equation 5 [Kaufmann, 2008].

$$A(c) = \alpha_1(1 - \exp^{-\alpha_2 c}) \quad (5)$$

Three known sodium dilutions are used in order to make the fit. From the alpha coefficients I can then calibrate the intensity levels to a concentration in ppb by Equation 7.

$$\Delta_I = \frac{I_0}{I_1} \quad (6)$$

$$c = \frac{\ln(1 - \frac{\log_{10}(\Delta_I)}{\alpha_1})}{-\alpha_2} \quad (7)$$

The sodium concentration acts almost linearly with respect to absorption up to around 100ppb. Hereafter a slight curve is introduced which is therefore taken into account in Equation 7. During measurements a problem with noise occurred, and it seemed as if the sensitivity of the measurement was bad. This could be caused by the enzyme being too old, but looking into the Limit of Detections, LODs, (see Section 4.2) of the standard runs values around 2.7ppb are observed which is considered acceptable compared to earlier measurements of sodium in for instance Dome C. Here the Eemian data has an LOD of 2.6ppb, and the overall data has an LOD of 3.6ppb (pers. comm. M. Bigler). This makes me believe that the column material is still okay. This material consists of an enzyme that with time will be less sensitive. Especially contact with water can affect the enzyme, and this is quite difficult to avoid completely.

During my Eemian measurements a flowcytometer was implemented in the system. This is done with the input of more lines and an extra peristaltic pump, and my guess is that this would perhaps cause some sensitivity changes. I do not know how much influence it would have, and if it is actually noticeable in the sodium measurement.

Abakus - a particle detector

The measuring of dust is done with a particle detector. The detector uses a laser beam to determine the particle size. The sample water passes through a flow cell with this beam, and the attenuation of the particles are then measured. This way the size of the particles can be detected. A calibration of size is usually done by the use of a comparative measurement with a Coulter Counter¹³, but in my results this calibration was not done.

A calibration of the dust results are necessary for comparison with other data. The Abakus produces results in $\frac{\text{particles}}{\text{second}}$ and I want $\frac{\text{particles}}{\text{mL}}$. The transform is given by:

$$\frac{\text{dust}[\frac{\text{part.}}{\text{s}}] \cdot 60}{x[\frac{\text{mL}}{\text{min}}]}, \quad \text{x=dust flow} \quad (8)$$

¹³A Coulter Counter uses micro channels that separate two chambers containing electrolyte solutions. When a particle passes through, the resistance of the liquid filling the micro channels is changed. This change can be recorded as electrical current which then tells about the particle size.

where the dust flow in my case is $2.25 \frac{mL}{min}$.

Conductivity instrument

The conductivity is measured by a conductivity meter connected to a micro flow cell. A conductivity meter uses a potentiometric method and is usually constructed with four electrodes. An alternating current is applied to the outer pair of electrodes, and the potential between the inner electrodes is measured.

The definition of electrical conductivity is a substance's ability to conduct an electrical current. An electrical current will form when a potential difference is placed across a conductor. Therefore the conductivity is a measurement of the ionic constituents in the ice including both positive and negative ions compared to the ECM which predominantly measures the amount of H^+ .

4.2 Resolution

Temporal resolution

An important factor when analysing ice cores is to have a good temporal resolution. This resolution can be studied by looking at the response times for the different components when acting on a standard measurement. In Figure 24 a comparison of the response of ammonium and conductivity when subjected to an ammonium standard solution is shown.

It is obvious that there is a difference in the resolution in this case. The temporal resolution is defined as the time required for the signal of a step function to rise from 10% to 90% of the final height [Kaufmann, 2008]. A step function is in my case a switch from blank to the standard solution. From the temporal resolution the depth resolution for the different components can be calculated from the melting speed (in my case approximately $1.5 \frac{cm}{min}$).

I have in Figure 25 used a measurement of a multi-standard. The top plot just shows that the resolution does not depend on the concentration of the standard. The three lines indicate the different time spans, the multi-standard was injected during, and clearly the resolution is almost the same since the shapes of the peaks are the same. The middle plot shows the temporal resolution difference in conductivity, ammonium, and sodium. Conductivity (green) is seen to have a very fast response to the standard.

Finally the bottom plot shows the resolution differences between the standard put between two mQ ice cubes and then melted (s1) and the standard injected directly via the master valve (s2). In this case, I would expect a

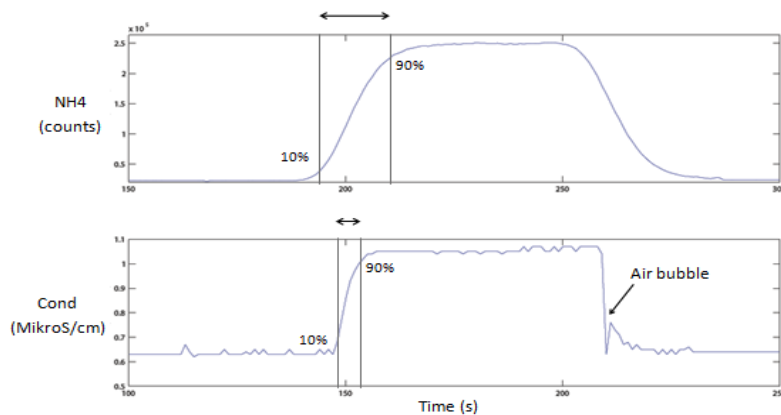


Figure 24: A comparison of the temporal response of a standard solution seen in ammonium and conductivity. The vertical lines indicate 10 and 90% of the increase of the total concentration level respectively. The difference in temporal resolution for the two components is easily seen. Both plots are shown on a 150 second interval.

big difference in resolution due to the ice going through the melting device where mixing of the fluids occurs. But actually the difference is not so big which leads me to think that it is not as important. Another part of the system, where mixing happens is, in the debubbler. The debubbler has a rather big volume compared to the tubings and other parts, and therefore I imagine that a great deal of dispersion happens here.

The three plots are all normalised to 1 for comparison of the resolution since the dispersion does not depend on the concentration used in the standards. The shape and steepness of the peak tells me about the resolution of the data [Rasmussen, 2005]. A very steep curve with sharp edges is best since this means that the instrument quickly responds to the standard and quickly gets it out of the system again. The quicker the response, the more narrow peaks can be observed when measuring real ice.

An additional usage of this multi-standard is to determine the time span between the different instruments' response to a given sample. This will be used in the data processing.

Figure 26 shows a comparison of the KUP setup and the CIC setup in the spatial spectrum¹⁴. We clearly see a difference in the shape of the peaks where the CIC resolution is better than the KUP resolution, but here we

¹⁴Voltage and counts are linearly dependent so no calibration is required

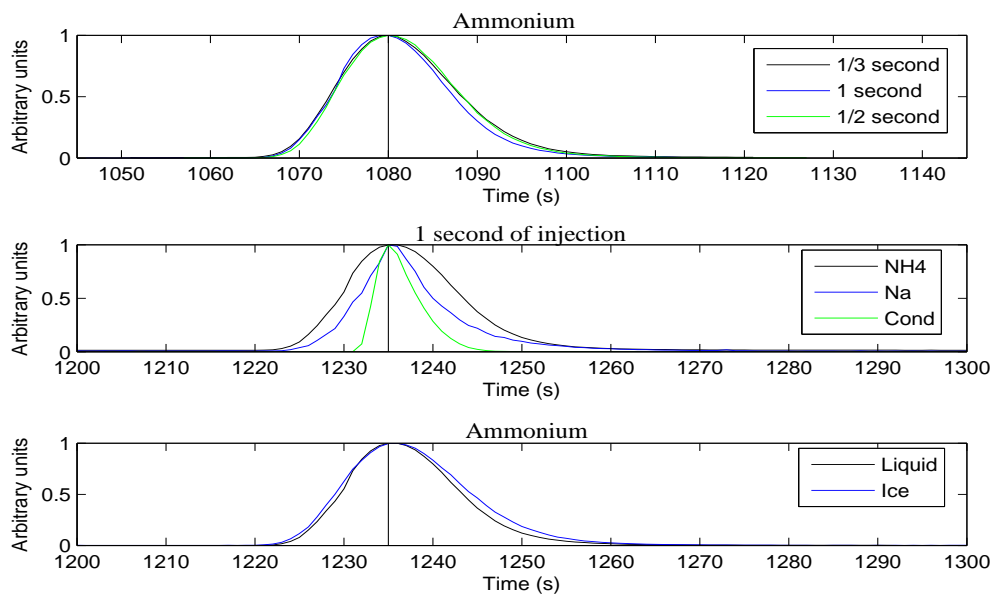


Figure 25: Top panel shows the temporal resolution for 1/3, 1/2, and 1 second of injection of an ammonium solution. Middle panel shows the response of NH_4^+ , Na^+ and conductivity to a 1 second multistandard solution. Bottom panel shows the resolution compared between a liquid solution and a standard between two mQ ice cubes. All peaks are standardised to 1, and the abscissas all equal an interval of a 100 seconds. The peaks are centered around the maximum value.

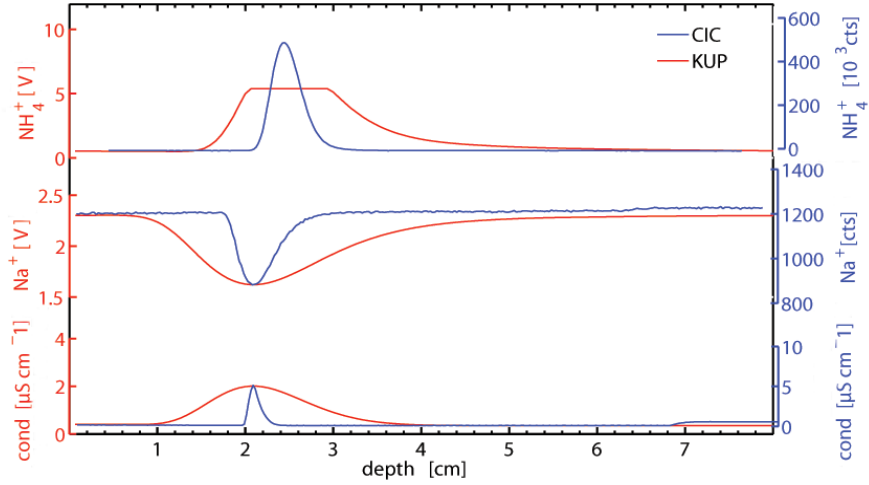


Figure 26: Spatial resolution comparison of the KUP setup with a flow rate of $4.0 \frac{cm}{min}$ and the CIC setup with a flow rate of $1.5 \frac{cm}{min}$. The CIC resolution is seen (from the shape of the peaks) to be higher than the KUP resolution, but mainly due to the different flow rates. The ammonium component in the KUP setup has reached maximum voltage, and I have therefore tried to give an estimate of the top of the peak.

have to take into account the fact that in Bern they measure ice with a higher melting speed which of course affects the resolution. To compare the two setups on a fair basis, I tried to make this plot with a melting speed of $4.0 \frac{cm}{min}$ for both setups. This results in a plot as seen in Figure 27. Here we actually still see a difference but not as distinct as before. This makes me think that the resolution difference is mainly caused by the different melting speeds. The conductivity resolution, however, is still much higher in the CIC setup.

Deconvolution

As the resolution is limited by the geometry of the melting device and the debubbler, and the turbulent mixing in the different parts of the setup, high frequency signals in the ice can be lost. With the use of a deconvolution technique, some of these cycles can be restored [Rasmussen, 2005]. Unfortunately this only includes the mixing that happens in the analysis part of the setup; it does not include the mixing happening in the melting device or the debubbler.

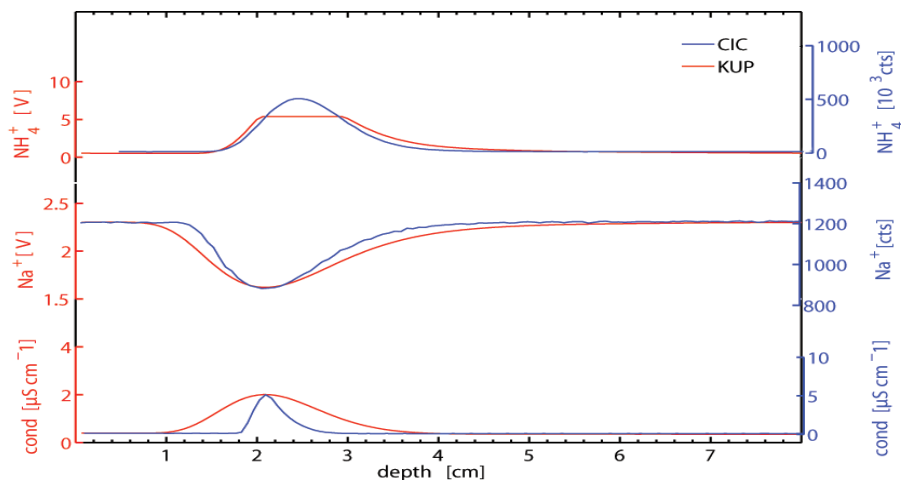


Figure 27: Spatial resolution comparison of the KUP setup with a flow rate of $4.0 \frac{cm}{min}$ and the CIC setup with a flow rate of $4.0 \frac{cm}{min}$. The CIC and KUP resolution is seen to be almost similar except for the conductivity signal where the CIC setup resolution is still quite higher. The ammonium component in the KUP setup has reached maximum voltage, and I have therefore tried to give an estimate of the top of the peak.

As seen in Figure 25 the conductivity signal has the fastest response to a multi-standard injection. The conductivity measurement contains less tubing and no mixing or reaction coils which results in less dispersion. The mixing in the conductivity sample can therefore be regarded as an estimate of the maximum mixing taking place in the melting part of the setup and in the debubbler.

To incorporate these parts in the deconvolution, a measurement of perfectly clean ice with a uniform concentration should be used, and such ice is not available from natural sources or by self production. The clean ice should also have a clean air content that is similar to that found in ice cores so that the sample-to-air ratio is the same and hence is comparable to real conditions. So far the deconvolution method has therefore only been used to restore data lost in the other mixing volumes in the setup.

Limit of detection

The limit of detection describes a measure of how weak a signal you can record with your instrument. It is a way of determining whether you can

distinguish a given substance from the signal value of a blank substance. Detection limits are defined in terms of error.

The detection limit is estimated from the mean of the blank, the standard deviation of the blank, and a confidence factor [Harsham 1995, ACS Comm 1980]. Different kinds of detection limits exist. These are:

- IDL: Instrument detection limit

This limit is defined as three times the standard deviation of the blank. Physically the IDL is the concentration required to produce a signal greater than three times the standard deviation of the noise level.

- MDL: Method detection limit

The more steps involved in a measurement the more errors there will be. If all steps are included, the detection limit is called MDL. An easy way to measure this limit is to take the dilution of the substance multiplied by the IDL. This will underestimate the MDL since no account is taken to the preparation steps.

- LOQ: Limit of quantification

The LOQ determines at which limit we can differ between two different values of a substance. Mostly the PQL¹⁵ is used. This limit is five times the LOQ which accounts for the fact that most laboratories are different.

Detection limits depend on both noise level and signal strength. Therefore it is of utmost importance to improve the signal to noise ratio. In my measurement the IDL is used when for instance comparing the sensitivity of the sodium column material to earlier measurements as mentioned in section 4.1.

4.3 Data processing

The raw data from the data acquisition needs to be calibrated and adjusted into usable results. Aligning the components is necessary because the different instruments receive the sample water at different times. This procedure is quite simple. By using a multi-standard solution it is easy to detect and calculate the difference from the sample entering one instrument to another. This difference turns out to be the same from measurement to measurement within a few seconds. These couple of seconds can be ignored since 2 seconds

¹⁵Practical Quantitation Limit

correspond to approximately half a millimeter of ice which is negligible in my measurements.

Besides the alignment, a calibration of each component except conductivity has to be made. The conductivity measurement already produces the data in the desired unit which is $\mu\text{Siemens}$ per centimeter. The calibration of sodium and ammonium is made with the use of standard solutions as described earlier.

During my measurements plenty of undesired situations happened. These were for instance when the ice got stuck on the melting device which produced air in the system, when small air bubbles was not caught by the debubbler, and finally when the encoder jumped; producing problems with the depth calibration. Often the ice got stuck when a break in the core section occurred. This also led to contamination of especially the dust signal. These problems need to be manually adjusted for in the data processing. This introduces errors in the results due to the fact that it is difficult to do very accurately, but it should not have an effect on the overall picture. Contaminated ice turned out to be a big problem, and I had to remove much data because of this.

A big issue with removing data is when looking for annual layers. In this case it is best to have a full set of data in order not to miss any years. The ammonium signal showed clear annual layers and was very unaffected by things like contamination and air in the system. Sodium on the other hand seemed to behave very badly. During measurements the baseline almost always drifted, and sometimes the level of the baseline was higher than the background concentration in the ice cores which produces negative results. The dust record also showed clear annual cycles but was easily contaminated by core breaks. Conductivity showed the nicest temporal resolution but is a measurement of a sum of different impurities and does therefore (at least in the Holocene ice) not show annual cycles.

In the first 10 bags, from interval 1A, I measured, a big problem was too many air bubbles in the system. Air bubbles especially messed up the conductivity measurement. With that many data points needed to be removed, it will be too time consuming to do manually; therefore I used Matlab to find sharply declining data points instead and eliminate these. That worked quite well.

Problems with the ice core getting stuck during the measurement was, on the other hand, easy to adjust for because the encoder stood still at that time, and the problem was thus removed when calibrating the encoder to depth scale.

The depth scale is calculated from the encoder data as described in sec-

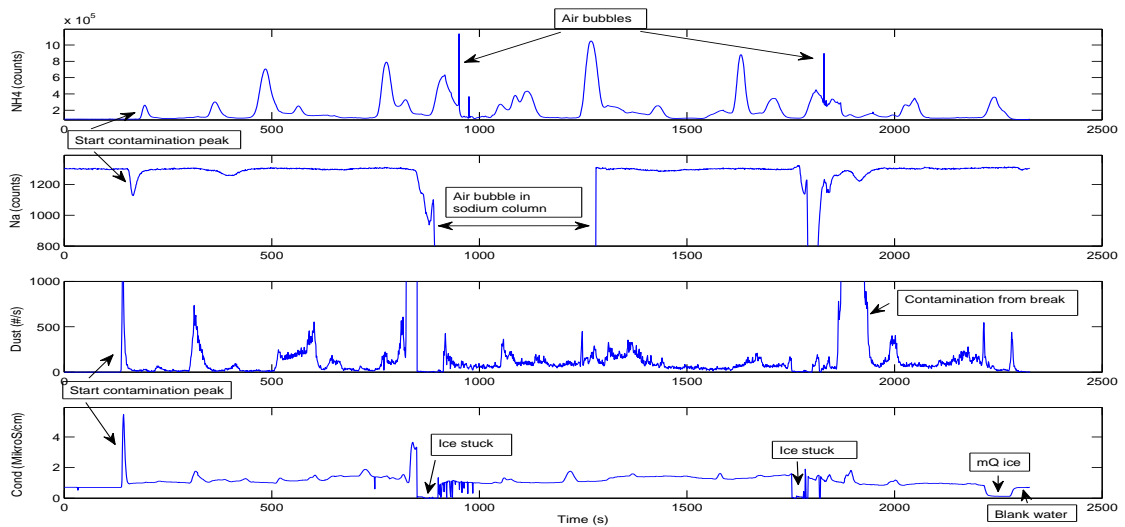


Figure 28: A plot of my raw data. Some of the problems are shown with arrows, but more exists.

tion 4.1. This depth scale has random step values, and therefore I made a depth scale with one millimeter intervals which is also necessary for making fourier analysis. Figure 28 shows an example of my raw data, and Figure 29 shows the processed data.

Power spectre

I am interested in determining the temporal resolution of my dataset for which I will use power spectra. These can give an estimate of how thin annual layers the measurement will resolve, for instance if it will be possible to identify annual layers in the Eemian ice, assumed that they still exist. The layers can be twisted and out of chronological order because of bottom topography and other disturbing processes.

At first I had to remove the data with no information. The gaps are then interpolated linearly to make a complete dataset which is required to make a discrete fourier transform. A discrete fourier transform transforms a function from the spatial domain to the frequency domain which helps identifying the dominant frequency in the signal. This dominant frequency would equal the annual cycle and hence give an estimate of the layer thickness in the given section. I use the built-in fast fourier tranform “fft” in Matlab to do this

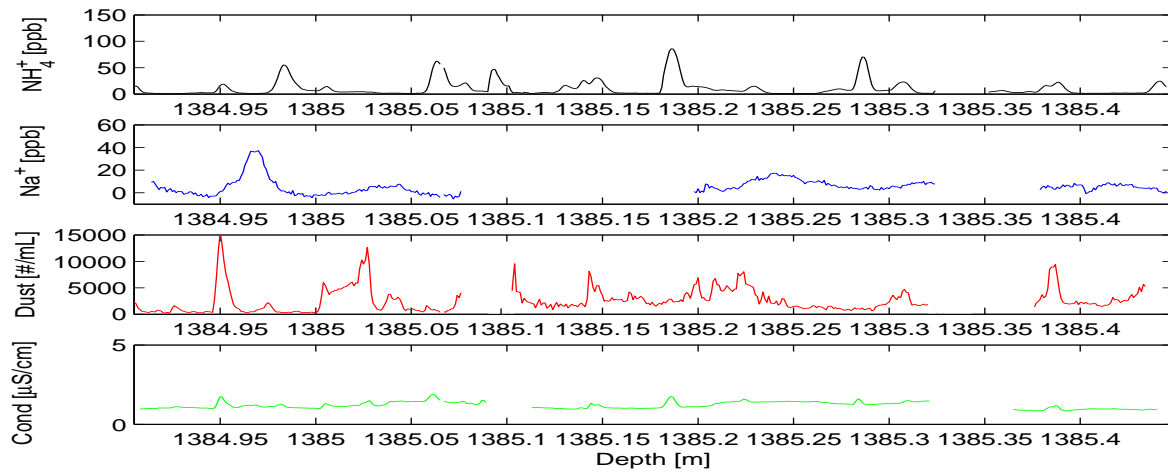


Figure 29: A plot of my processed data after aligning components, calibrating to concentration and producing the depth scale. Air bubbles are removed as well as contaminated parts and when the ice is stuck. Gaps arise due to breaks in the core or contamination.

calculation. The spectrum is cut off at the Nyquist frequency which is given by $\frac{1}{2 \cdot \Delta t}$ where Δt is the resolution of the data - in my case $1mm$. The Matlab code is:

```

Y = fft(NH4_interp)
Y(1) = [ ]
n = length(Y)
power = abs(Y(1:floor(n/2)))^2
nyquist = 1/(2*0.1)
freq = (1:n/2)/(n/2)*nyquist

```

I remove the first value in the fourier transform since this is just the sum of the data. In the power equation, I use only half the fourier spectrum since the result, when calculating a fourier transform, is symmetric around the frequency $\frac{n}{2}$.

5 Results and discussion

5.1 The Holocene profile

In Figure 30 a section of my results is shown. 5 bags are shown in the depth interval $1381.05m$ to $1383.80m$. The black curve is ammonium, NH_4^+ , the blue is sodium, Na^+ , the red is dust, and the green is conductivity. (The rest of the Holocene results are in Appendix B.)

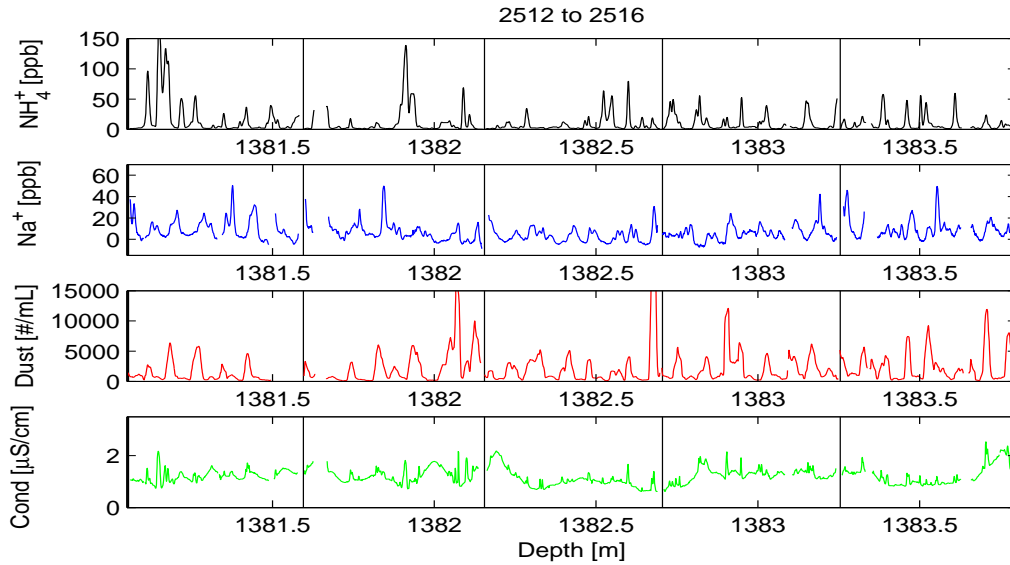


Figure 30: CFA profile of bag 2512 to 2516 (Depth interval: $1381.05m$ – $1383.80m$). Vertical lines indicate separation of bags.

As the reader may notice the sodium values sometimes drop below zero. This is of course not an acceptable result since negative concentration values do not make sense. These values are due to a blank level lower in intensity than the actual measurement. I will keep the negative values during the presentation of my results, but I will come back to this issue in the end of the section. The results show good annual variability in ammonium, dust, and partly in sodium.

Conductivity is a bulk signal, and in the warm periods it is difficult to talk about seasonal variation in the this signal¹⁶, but we clearly see some broad, significant peaks in the conductivity profiles. When comparing these

¹⁶At least not in the Holocene period. Whether this is also true for the Eemian, I will discuss later.

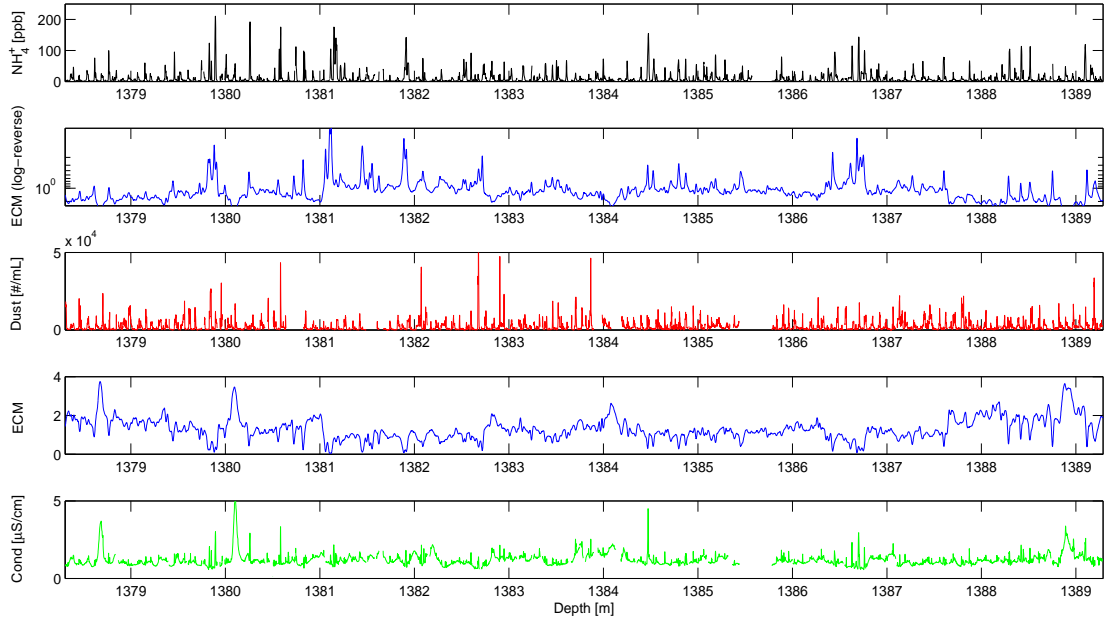


Figure 31: Comparison of ECM with the Holocene CFA profile. From the two top panels an anti-correlation of ECM with the largest peaks in NH_4^+ can be drawn. Note the reversed ECM scale. From the two bottom panels a correlation between ECM and conductivity can be drawn.

to the ECM profile, a correlation is clear. ECM is an acid-signal, as it measures mainly H^+ ions, so we would expect the large peaks to originate from sulphuric acid, H_2SO_4 , among others. This would indicate that the large spikes come from volcanic eruptions. The overall trend (low frequency variation) also seems to be the same in conductivity and ECM. Since conductivity is a bulk signal of all ionic constituents, both positive and negative, I would expect it to have some wiggles that are not seen in the ECM signal. (See Figure 31). Besides the broad peaks, the conductivity signal has a lot of narrow peaks which often coincide with peaks in ammonium probably caused by major forest fires or peaks in dust originating from extensive desert storms.

Dating of the Holocene section

In my Holocene profiles I definitely see seasonal variations in both ammonium, sodium, and in dust. Often we see peaks in conductivity that are comparable to the dust peaks. This is probably due to the soluble dust in form of calcium, that conductivity measures. As mentioned in section 2.1, during warm periods the different ionic impurities peak at different times, unlike during the glacial where the different ionic components peak almost at the same time which makes it possible to use as well conductivity for annual layer counting.

One of the purposes of this thesis is to date the ice from the intervals, I have measured. I have two approaches to this issue. From a fourier spectrum of the profiles, the dominant frequency can be determined and hence give an estimate of the amount of years in a given section, but when actually dating an ice core the seasonal variation peaks are simply identified and counted. As the fourier approach gives an estimate of the annual layer thicknesses, and as this parameter changes with depth, it will therefore only be an estimate of the number of years. Often this method will not give a usable result since the annual peaks can be lost in noise.

In Figure 32 the fourier spectrum of the results from bag 2517 to 2526 is shown. The procedure is described in section 4.3. An annual peak is seen at around $7.69 \frac{cm}{year}$.

In Figure 33 a section of my counting is shown. The grey vertical bars mark the peaks in ammonium so the phasing between the components are clearly seen. Sodium peaks are in between the ammonium peaks, as this is a winter signal, and dust peaks are right before (as seen on a time scale) the ammonium peaks, as this is a spring signal.

My total dating results are summed up in Table 1. The counting I trust the most is the one made with the use of the ammonium record since this signal seems to be the most robust (and most unaffected by contamination). A comparison with GICC05 is also listed. As my annual layer thickness estimate from the fourier analysis was $7.69 \frac{cm}{year}$, it fits well with the estimate from Table 1, as $\frac{1100cm}{145 \pm 1yr} = 7.59 \pm 0.05 \frac{cm}{year}$.

Baseline trouble in the absorption measurement

Negative sodium concentrations are not an acceptable result, and these values are caused by a wrong level of blank water in my measurement. When measuring a bag, blank water is measured before and after the ice sample. This blank water is assumed to have a concentration of zero ppb of the im-

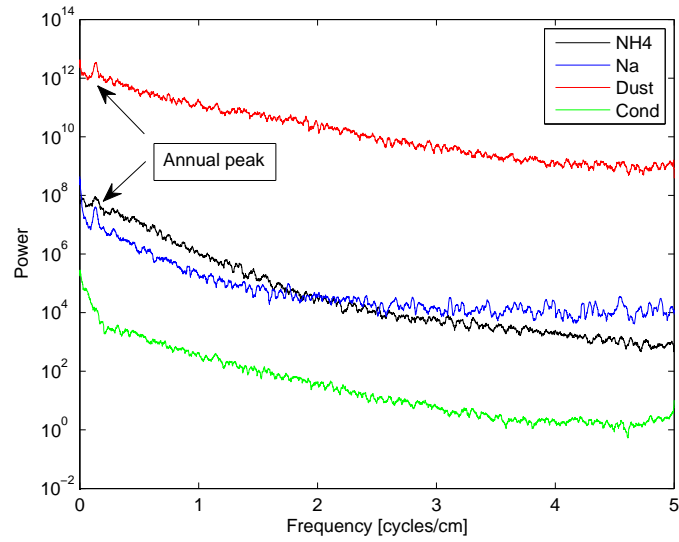


Figure 32: Power spectrum of bags 2517 to 2526. The annual peak is seen at around $0.13 \frac{\text{cycles}}{\text{cm}}$ which correspond to approximately $7.69 \frac{\text{cm}}{\text{yr}}$.

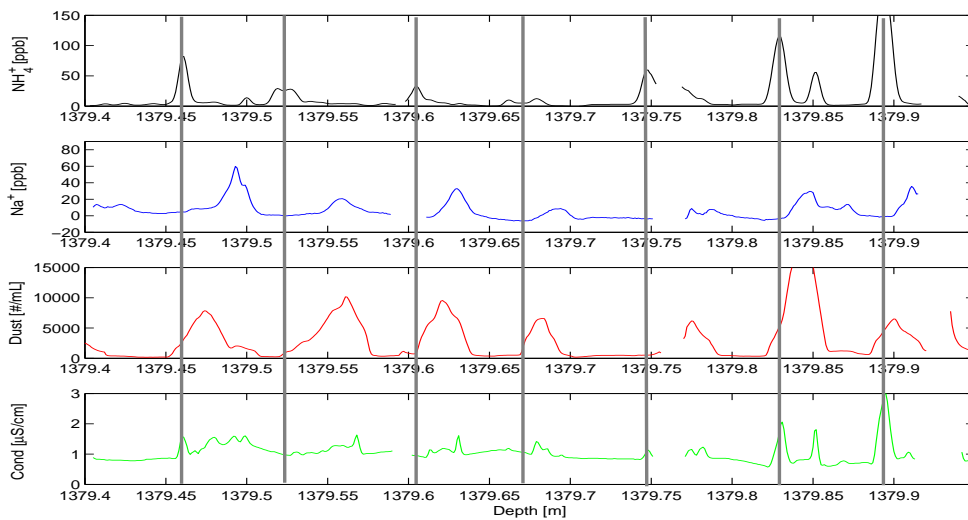


Figure 33: A section of my dating from bag 2509. Grey vertical bars mark the annuals observed in the ammonium peaks. The phasing of the seasonality of the components is clearly seen.

	2507 to 2511	2512 to 2516	2517 to 2521	2522 to 2526	Sum
NH_4^+	35	37	35 ± 1	38	145 ± 1
Na^+	35	35	34.5 ± 1.5	-	-
Dust	34	37	36 ± 1	38	145 ± 1
GICC05	36	37	36	37	146

Table 1: Annual layer counting of the Holocene period. All values are in years. The uncertainty estimate is obtained from identification of “uncertain” annual layers which are weighted by a half and with half a year uncertainty. Sodium values from bag 2522 to 2526 were affected by contamination and do not count in the result.

purities in question and is used in the calibration. Therefore it is a problem to have a blank level with a lower intensity, i.e. higher concentration, than the actual background level of the ice. See Figure 34 for an example of a blank level lower in intensity than the measurement. The red line indicates my interpolated blank level in the given calibration.

A solution might be to interpolate a baseline with the use of the background intensity of the ice, but this, I estimated, would be too time consuming compared to the gain. In Figure 34 a drifting baseline, which of course is not good either, is also seen.

If we assume that these negative values of sodium are caused by something with our blank water and not something with the actual measurement

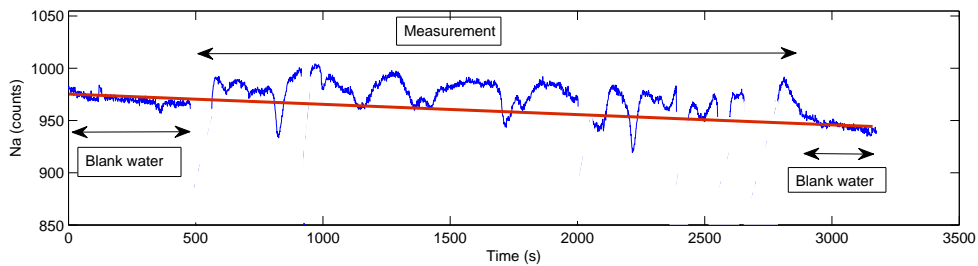


Figure 34: Raw data plot of sodium. The red line indicates the blank level in the shifts from the beginning to the end of the measurement, and how this level, when interpolated, is lower in intensity than the actual measurement. Contaminated parts are removed.

	Means KUP	Means CIC	Median KUP	Median CIC
NH_4^+ [ppb]	15.3	10.6	7.03	3.82
Na^+ [ppb]	16.3	4.9	14.7	3.97
Dust [#/ <i>mL</i>]	9400	2400	6900	1100
Cond [$\mu S/cm$]	1.3	1.21	1.1	1.12

Table 2: Means and medians of the four components in the KUP and CIC setup. KUP (1405*m* to 1420*m*), CIC (1378*m* to 1389*m*) Medians are listed since these values downgrade the influence of large peaks in the records, and therefore might be more reasonable to compare between the two setups.

of the ice, then a possible adjustment of the results would be to just change the level of zero. This can be done with earlier CFA records of sodium from the Holocene ice if we assume that the levels are more or less constant within a hundred meters or so. Table 2 shows the means and medians of sodium, ammonium, dust, and conductivity measured with the KUP setup. Depth is from around 1405*m* to 1420*m*.

If I try to adjust my sodium levels with the use of the results listed in Table 2, I get a profile as in Figure 35. This is an acceptable result but it tells me that my sodium results are not good when studying absolute values. It can still be used for dating purposes though.

Another problem with the sodium results is the drifting baseline. With an appropriate baseline (assuming that the ice measurement itself drifts along), this drift will probably not be seen in the calibrated results. It should still try to be avoided though. There should be no drift in the measurement at all so this tells me that something in the setup must have an influence on the signal. During measurement there was often problems with air in the flow cell where the absorbance of the sample is measured. This air usually resulted in an unusual drop in intensity, and when the air had passed through, the intensity level would go back to normal. Although sometimes, in spite of the removal of an air bubble, the intensity level did not jump back to the initial level. This is one explanation of why my baseline could be at another level after measurement, but often it was clear that the baseline just drifted.

The drift might be explained by pressure problems in the setup. The CIC setup differs from the KUP setup in where the peristaltic pump is located. In Bern it is located just after the melting head, and the sample is therefore pumped through the different channels. In Copenhagen we have it after some of the components and before others. This means that the sample is sucked through the distributor. This construction will unfortunately result

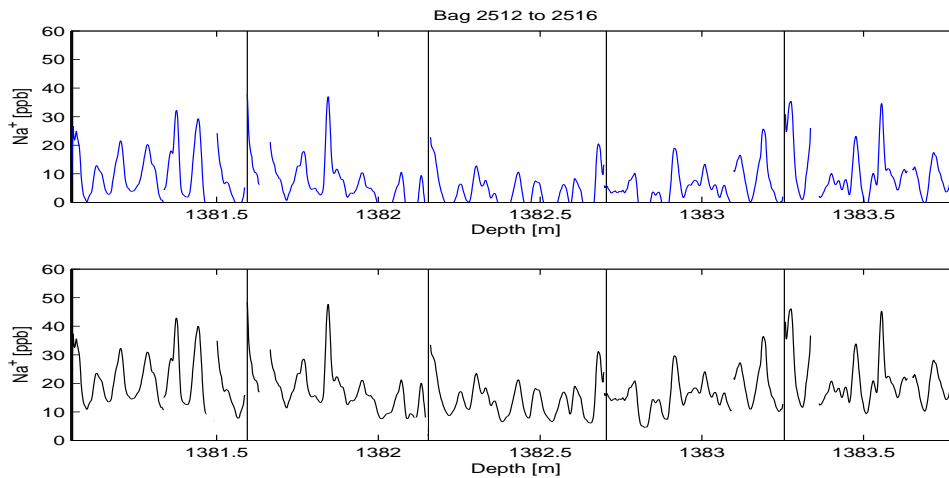


Figure 35: Sodium record from bags 2512 to 2516. Top panel shows the sodium signal after calibration to concentration. The background level is sometimes below zero. Bottom panel shows the same calibrated record when adjusted according to the mean level of the KUP data.

in an effect on the other components if one component experiences problems. Because we wish to avoid a melting pump in order to get a shorter distance from the melting to the measuring unit, we have to have a closed system in Copenhagen. This means that we do not have an excess pressure release in the debubbler. If pressure builds up in the system, then a leak of pressure from whatever tiny holes there inevitably will exist will influence the signal. If this happens during measurements, I would imagine that it could result in the drifting baseline. We have also not got a temperature stabilization of the detection instruments in Copenhagen either, and if the ambient temperature changes during a measurement, this might affect the sodium signal. The sodium signal is more sensitive to temperature changes than ammonium, and the optimum operation temperature for sodium is 16°C [Kaufmann, 2008].

Dust differences from one setup to another

Table 2 also shows a difference in dust level between the two setups, but there also exists a difference compared to the new KUP setup. The old CFA setup has a mean concentration of around $10.000 \frac{\#}{mL}$ [Ruth, 2003], the new KUP setup has a mean of around $100 \frac{\#}{mL}$ [Kaufmann, 2008], and my results give a mean of around $2.500 \frac{\#}{mL}$. I have not been able to find the

exact explanation of these differences, but investigation of the results and repeated calculations seem to point at a difference in measurement methods. With the old setup the detection limit was not so well defined, and the size distribution measurements were done with only a few quite large size channels (pers. comm. M. Bigler). This might explain the difference in level also considering the relatively low interglacial values.

The new and old KUP CFA setup seem to simply differ by a factor of 100 when looking at peak and background levels as these are around $300 \frac{\#}{mL}$ versus $30.000 \frac{\#}{mL}$ and $20-30 \frac{\#}{mL}$ versus $2.000 \frac{\#}{mL}$ respectively. This can not be the case when comparing the old KUP setup with the CIC setup. The CIC setup has a background level of around a $100 \frac{\#}{mL}$ which is much lower than the level from the old CFA setup, but my peaks reach values of $20.000 \frac{\#}{mL}$ where the old CFA setup have peaks up to $30.000 \frac{\#}{mL}$ so from this, I can conclude that it is not only a factor of difference between these two setups. With the CIC setup a calibration from a Coulter Counter is not done, but I have not found the direct influence of this calibration anywhere, although according to Ruth et al. [Ruth, 2003] it only had an influence of around 5%.

5.2 The Eemian and Early glacial profiles

In this section I will present the results I have obtained for the Eemian–Early glacial periods. As I have measured four bags at each location, which correspond to $2.2m$, this number of bags may not be enough to get a full picture of whether annual layers are preserved or not, but it can give me an idea of how the concentration levels of impurities were during these time periods.

Eemian CFA records

In Figures 36, 37, and 38 the profiles from the three intervals are shown. These results clearly show a different peak behavior than the Holocene profiles.

As we are now at almost $3km$ depth, the annual layer thicknesses according to ss09sea are around $1cm - 1.47cm$. This results in a higher frequency of peaks in the impurities, but — as obvious to the reader — it does not seem this way in ammonium for one. The Eemian ice was visibly very different from the Holocene ice. Since the ice has been located so close to the bottom and thus been more warm due to geothermal heat, ice crystals have had the possibility to grow very large.

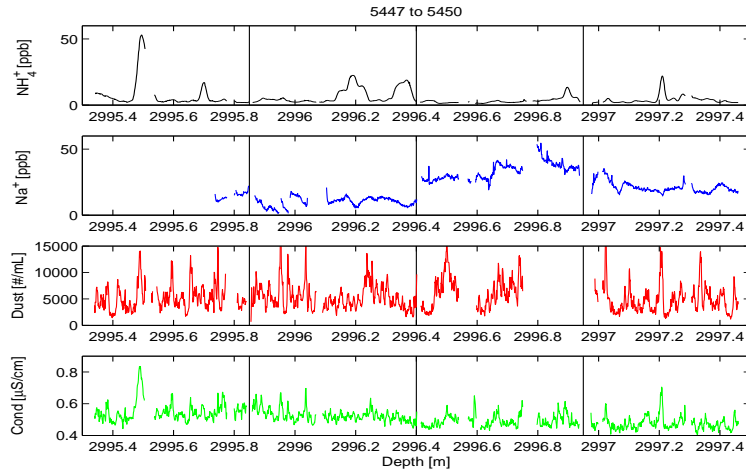


Figure 36: Profile of interval 1B. Vertical lines indicate the separation of the four bags measured. Contaminated data has been removed, as well as breaks in the ice core which result in data gaps.

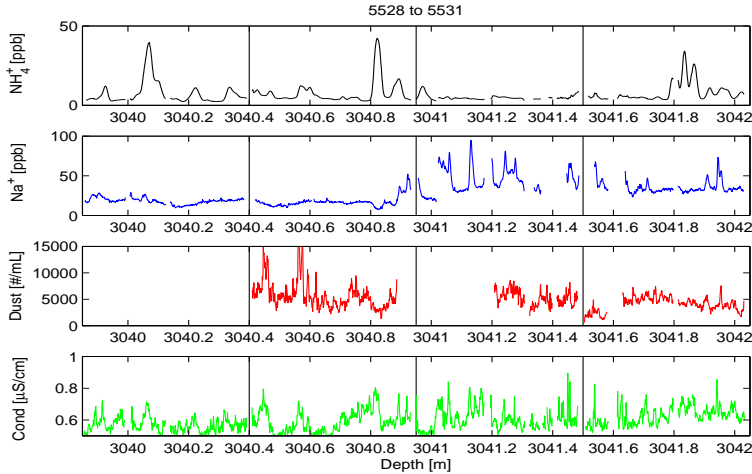


Figure 37: Profile of interval 2B. Vertical lines indicate the separation of the four bags measured. Contaminated data has been removed, as well as breaks in the ice core, which result in data gaps.

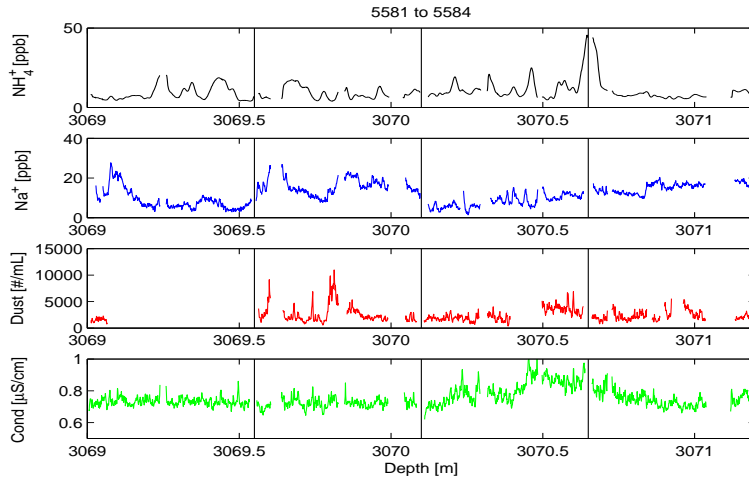


Figure 38: Profile of interval 3B. Vertical lines indicate the separation of the four bags measured. Contaminated data has been removed, as well as breaks in the ice core, which result in data gaps.

An interesting element in the sodium measurement is the results for interval 2B. In this profile an unusual jump in level happens between bag 5529 and 5530 (See Figure 37). The increase actually already happens during the end of bag 5529. If the jump was right between the two bags, I would assume that something had changed in the system, and that the data should be disregarded, but since this is not the case, I would think that it is a true signal in the ice core although it might also be some sort of contamination problem. During the Eemian–Early glacial measurements we had a lot of problems with drilling liquid in the dust measurement¹⁷, but this problem they also had in the Dome C¹⁸ measurements, and here they experienced no effect on the chemicals (pers. comm. M. Bigler) which makes me discard this explanation.

If we look at the $\delta^{18}\text{O}$ climate behavior in just this section, we see a shift in $\delta^{18}\text{O}$, albeit small. See Figure 17 on page 22. Unfortunately the shift is towards higher $\delta^{18}\text{O}$ values with depth which would suggest a smaller amount impurities, and what we see is a higher amount of impurities. Also remarkable is that, where sodium peaks in intervals 1B and 2B seem almost

¹⁷Drilling liquid was identified by looking at the size distribution where the same size particles showed up quite often and formed a certain S-shape in the distribution (Work by E. Kettner).

¹⁸Dome C was a ice core drilling made in East Antarctica.

smoothed out, there is a change in this behavior right at the level shift. The sodium shows more variations with rather distinct peaks as if it was not smoothed out right here, or maybe something else produces these peaks.

Dating in dust and conductivity

In the Eemian and Early glacial profiles we clearly see that ammonium shows no annual layering, and that sodium is not really reliable. Sodium has a lot of ups and downs in its background trend, and since the $\delta^{18}\text{O}$ does not have huge jumps, I then degrade the importance of this component in my further study. Left is dust and conductivity. In the Holocene ice, I concluded that annual layering is not seen in conductivity but zooming in on the profiles from the Eemian periods I see a clear correlation between dust and conductivity. (See figure 39).

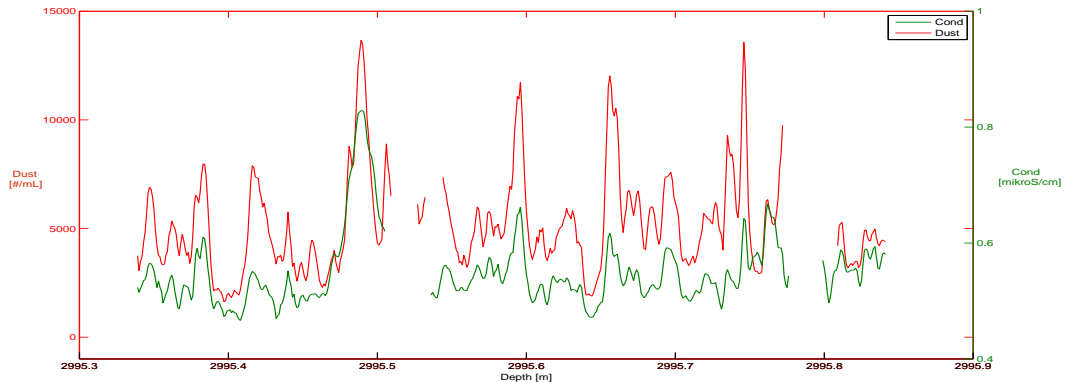


Figure 39: The plot shows the very distinct similarity between conductivity and dust. The data are smoothed with a running mean of 5mm.

As dust usually exhibits seasonal variations, I will trust that this is still true and assume that we also see annual layers in conductivity. It could be, that the bulk signal, that conductivity is, in this old ice consists of other amounts of the different ionic constituents and therefore could show annual layering as it does in the cold periods.

The level of conductivity is lower than in the Holocene, and the signal seems to have a different behavior. It has spikes both up and down where in the Holocene the peaks are mostly towards higher values superimposed

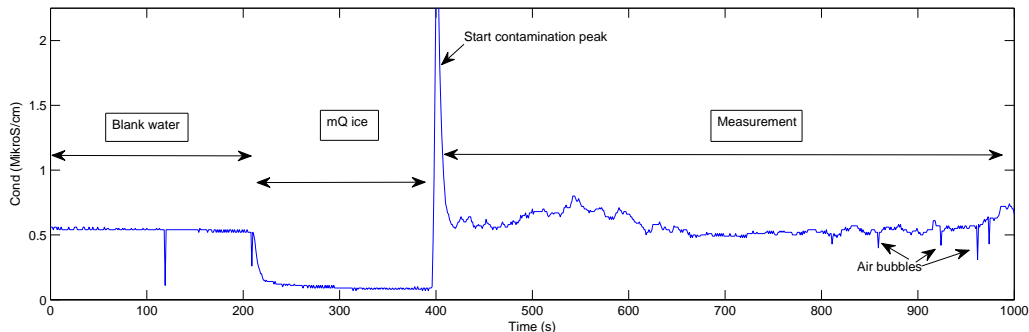


Figure 40: Raw data showing the wiggles in conductivity in the actual ice measurement compared to the ones in the mQ ice and in the blank water. This excludes the theory that the dust and conductivity signals are simply noise.

on a background level. This could indicate white noise¹⁹. One might argue that the whole signal is just a noise signal, but in Figure 40 a comparison is made between the blank level, mQ ice variations, and the signal itself.

Since the conductivity signal looks much like the dust signal, the two components must have something, that produces this signal, in common. Maybe it is just a pump signal, but this explanation is ruled out due to the periods of the wiggles. They are much longer than the pumping sequence. The wiggles have a period of roughly around 30 seconds, and my guess is that the pump has a period of half a second or so. Also the conductivity and dust have two different instruments and power supplies so there can be no electromagnetic interference. The setup specifications are totally independent; therefore I conclude that it must be a true signal from the ice.

As conductivity and dust are so much alike, conductivity could be dominated by soluble calcium in the ice that has not moved around and is not released until the ice is melted. This would explain the similarity with the insoluble dust. An interesting measurement would therefore be to have had a calcium measurement for comparison.

Assuming that we do see annual layers in the Eemian–Early glacial profiles, Table 3 shows my counting of annuals including uncertainties together with an estimate of the annual layer thicknesses. These values are then compared with the ss09sea results for these intervals. I would say that the

¹⁹White noise is a random signal or process with a flat power spectral density

	Interval 1B [$\frac{cm}{year}$]	Interval 2B [$\frac{cm}{year}$]	Interval 3B [$\frac{cm}{year}$]
Dust	$\frac{149.5}{153.5 \pm 8.5} = 0.974 \pm 0.057$	$\frac{103}{101 \pm 5} = 1.020 \pm 0.053$	$\frac{92}{63.5 \pm 5.5} = 1.449 \pm 0.137$
Cond	$\frac{198.5}{204 \pm 11} = 0.973 \pm 0.055$	$\frac{205.5}{213.5 \pm 10.5} = 0.963 \pm 0.05$	$\frac{194.5}{173.5 \pm 7.5} = 1.121 \pm 0.052$
ss09sea	1.07	1.19	1.47

Table 3: Annual layer counting in the Eemian and Early glacial intervals together with the corresponding annual layer thicknesses. The estimated annual layer thicknesses from ss09sea is also listed. In interval 2B and 3B, the dust values only include three and two bags respectively since contamination has affected the others too much. Especially the dust annual layer thickness estimate for interval 3B should be used with caution.

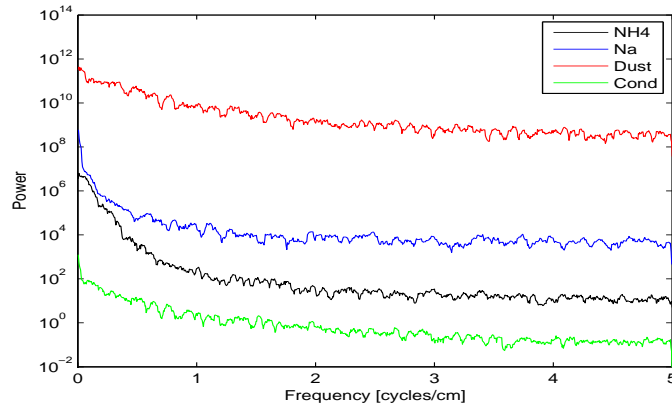


Figure 41: Power spectrum of interval 1B. The annual peak is not seen at all.

dating result is rather questionable and the fourier spectrum in this case shows absolutely no annual peak as seen in Figure 41.

Interval 1B has results comparable to ss09sea when including the uncertainties. Interval 2B results are a bit different from the ss09sea result, but in interval 3B the results are quite off compared to the ss09sea result when looking at conductivity. In interval 3B, contamination ruined almost all the dust data, and therefore the result should be used with caution, although it seems quite similar to the ss09sea result. My conductivity results for interval 3B, on the other hand, show more years than expected and hence thinner annual layers than suggested by ss09sea. The effect of this, I will come back to in my discussion.

6 General discussion

In this section I will discuss my results further. First I will give an estimate of the effect of the observed thinner annual layers in the Eemian period on the duration of the Eemian contained in the NGRIP core. Then I will give an overview and discussion of the levels of impurities during my measured climate periods together with the level around LGM. Comparisons of my impurity profiles with other results will also be discussed. This include resolution of the ammonium record compared to the calcium and ammonium record from the GRIP ice core, an explanation of low ECM values when large ammonium peaks occur, and a discussion of whether impurities — in this case ammonium — will move to crystal boundaries in the deep ice. Finally I will go through the improvements of the setup; what must be done and what could be interesting to look into.

6.1 Eemian annual layers and ss09sea

It is difficult to determine whether the annual layers detected in the Eemian ice are correctly observed or not, but below I have brought out pros and cons, and from this I will conclude that it is actually a true annual signal.

Pros

- The conductivity and dust signal in the Eemian period are very much alike. Almost every wiggle in one component can be, although sometimes weakly, seen in the other component.
- The two components are independent in instrument specifications so no common electromagnetic interference can exist.
- Conductivity was seen in the Holocene profiles to sometimes resemble the dust signal so maybe it could be possible that in the Eemian ice it resembles dust in almost every peak.
- The dating matches the ss09sea dating in two of the three intervals. Again it is only 2 consecutive meters for each interval and therefore a bias might be present.

Cons

- The conductivity does not look like the signal from the Holocene period because it goes both up and down and therefore more resembles noise.
- It seems unlikely that conductivity in the Eemian time period only will resemble dust peaks and not include large ammonium peaks for instance

— though this component is seen to be smoothed out to some degree at this depth, and therefore it would perhaps only add to the mean level of conductivity.

- The dating was quite difficult because it was hard to determine exactly which peaks were annual peaks and which were just noise.
- The fourier analysis showed no annual peak at all.

Whether I have dated this signal with the right amount of years or not is open for discussion. If I assume that my dating is correct, then Table 3 shows an interesting point. My estimated annual layer thickness, λ , fits okay well with the modelled thickness in interval 1B and 2B, but in interval 3B a difference of around $0.35 \frac{cm}{year}$ is noticed. This means that there will be more years from the Eemian period in the NGRIP ice core than estimated by ss09sea.

According to the ss09sea model the age at the bottom of the NGRIP core is 123.000 years. If I try to calculate the age at the bottom with a mean annual layer thickness of what I have observed for interval 3B in conductivity from 3069m (the start of interval 3B) to the bottom, I get an age difference of 328 years resulting in a total age of 123.328 years at the bottom.

The bottom melting at the NGRIP site is around 7mm ice per year which correspond to a geothermal heat flow of $140 \frac{mW}{m^2}$. This high geothermal flow is atypical for Precambrian shields that is believed to cover most of Greenland [NGRIP members, 2004]. Since the flow is considered unexpectedly high, it might be interesting to try and tune some of the bottom melting parameters in the ss09sea model for NGRIP to see if an annual layer thickness of around $1.1 \frac{cm}{yr}$ during the Eemian period can be obtained. This test is beyond the scope of this thesis though.

6.2 The atmospheric aerosol load through time

A comparison of my Holocene results with my Eemian and Early glacial results shows a clear difference. This is what I would expect since the ice from very deep in the ice core has been under a high pressure and exposed to more ice flow, as well as bottom melting, and bottom topography compared to the Holocene ice. This taken into account, it will therefore be interesting to study for instance concentration levels from the Eemian period to see if they are comparable to the present interglacial. As mentioned in the introduction, the Eemian was about 5°C warmer than the Holocene, and maybe the concentration levels of the impurities will reflect this in form of more extreme levels than the Holocene.

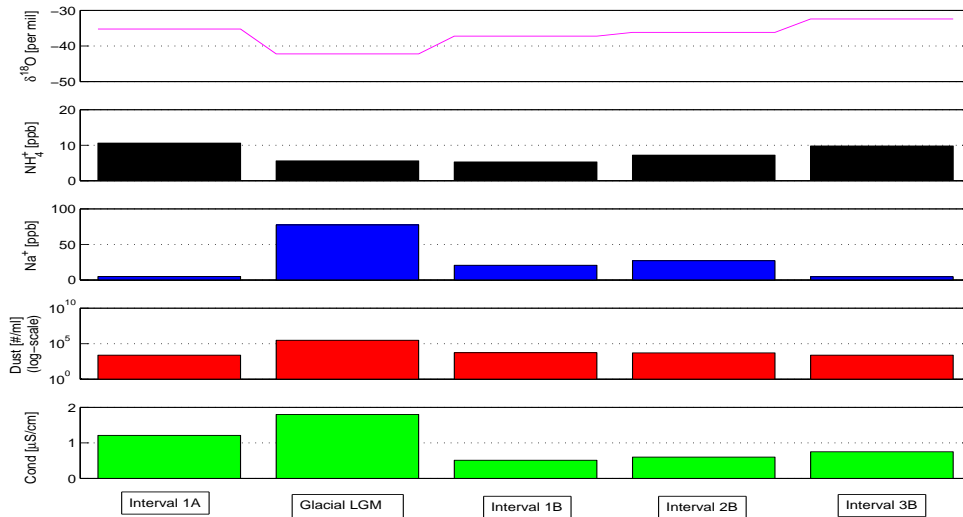


Figure 42: Mean concentration levels of the four components and including the $\delta^{18}\text{O}$ level for the Holocene, Glacial (LGM) and interval 1B to 3B. Note the logarithmic scale in the dust results.

I have in Figure 42 shown an overview of the levels of impurities found in the Holocene and in the three intervals from the Eemian–Early glacial. Table 4 lists the values of these levels. Glacial values are taken from earlier measurements made in Bern. As seen on the $\delta^{18}\text{O}$ values, the glacial is remarkably colder than the Holocene, and interval 1B is colder than the Holocene but warmer than the glacial. Interval 2B is almost the same as the Holocene, and interval 3B is warmer than the Holocene. I expected some kind of reflection of this in the impurity content. A short outline of the levels of the four components is given here.

- I still do not trust the sodium results, at least not when comparing to the glacial values. My sodium results have, as mentioned earlier, negative values, and the mean therefore does not make as much sense to look at. It will be lower than expected.
- The ammonium levels show a trend of higher levels with temperature. It is increasing from interval 1B to interval 3B, but it does not actually

	Interval 1A	Glacial	Interval 1B	Interval 2B	Interval 3B
$\delta^{18}O$ [per mil]	-35.22	-42.22	-37.22	-36.17	-32.40
NH_4^+ [ppb]	10.6	5.6	5.3	7.2	9.8
Na^+ [ppb]	4.9	77.5	20.8	27.13	4.7
Dust [#/ <i>mL</i>]	2.400	298.930	5.310	4.960	2.420
Cond [$\mu S/cm$]	1.21	1.8	0.51	0.60	0.75

Table 4: Mean level values of the four components including $\delta^{18}O$ as plotted on Figure 42.

go above the Holocene level which would be expected if the level depended solely on the temperature.

- The dust levels are very low compared to glacial values, and therefore I have shown this on a logarithmic scale. The Holocene and Eemian values are almost the same, and there is some trend that the colder periods, interval 1B and 2B, are a bit higher than 3B but still not at all in the same order as the glacial values.
- Conductivity shows an interesting trend. This component increases from interval 1B to interval 3B but is still lower than the Holocene level, and the glacial level is the highest.

A rule of thumb is that when colder, for instance during the glacial, the more impurities. This is true for sodium and dust, and the conductivity measurement shows the highest level as well during the glacial period. As especially dust is remarkably higher during the glacial, it is due to the more stormy weather bringing lots of desert dust to the Greenland ice sheet in these periods. Glacial values as for instance at LGM are a factor of around a 100 higher than interglacial values [Ruth, 2003].

The ammonium ion is the only component (in my measurement) that has a lower value during the glacial. In Fuhrer and Legrand 1997 [Fuhrer, 1997] a strong covariation between ammonium and the solar radiation at 60°N is mentioned. In Figure 43 insolation at 65°N through the last 900ka is shown. Ammonium as a respondent to insolation, continental bioactivity, and biomass burning has a direct temperature dependency.

The sodium values are rather unreliable because of their negative values, but it does show larger values during the cold, glacial period, which is to be

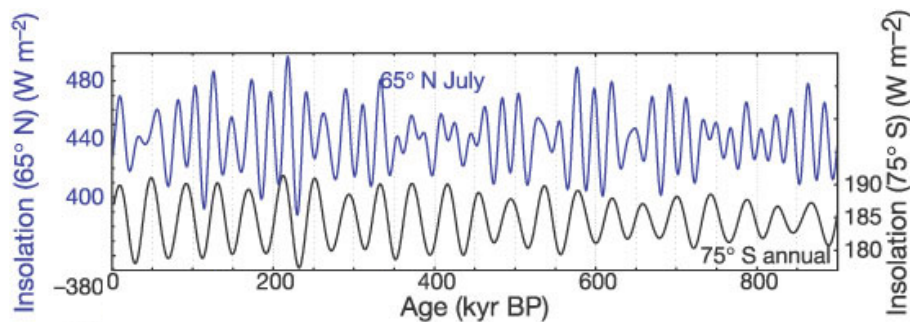


Figure 43: A comparison between the insolation at 65°N and 75°S during the last 800,000 years [EPICA 2004]. Ammonium is seen to correlate with the insolation [Fuhrer, 1997].

expected. The Eemian–Early glacial intervals on the other hand do not seem to have a temperature trend as interval 2B has higher values than interval 1B and interval 3B. This leads me to the conclusion that they can not be trusted very much with regard to concentration levels.

Finally when looking at the conductivity levels, it does not seem as straight forward as for the other components. It makes sense that the colder the more impurities and the higher a conductivity level we see, but then we see a temperature dependency as in the Eemian–Early glacial intervals. From intervals 1B to 3B the climate is warmer, and the conductivity increases, but it does not go above the Holocene, interval 1A, level. This could maybe be explained by combining two different variabilities of conductivity with temperature. When the climate is cold, it will be more stormy and dust is very well correlated with these storms and heavy winds. Some impurities tend to stick to dust, and this is what we call the irreversible species. These species are not volatile and will therefore stay on the ice sheet when deposited, despite a low accumulation rate. These impurities are for instance calcium, sodium, and ammonium (pers. comm. M. Bigler, 2009). This variability of conductivity produces an inverse dependence of conductivity with temperature.

Another variability of conductivity with temperature is caused by the reversible ionic species. If the temperature is high, we will see a higher accumulation rate. Due to a higher accumulation, the volatile species, such as chloride, nitrate, and methane sulphonate, will be sort of “buried” in the ice, and therefore will not escape. This results in a direct dependence of conductivity with temperature. The “volatile” term means that the species can react with other ions to form gaseous molecules, for instance can chloride

react with H^+ ions to form HCl . A reaction could be:



Having a variability of lower conductivity with higher temperature, we would see a trend that has a higher conductivity, the colder it is. This is part of what we see in the conductivity levels during the different time periods. We do have a higher conductivity level during the glacial compared to the Holocene, but in intervals 1B to 3B this does not hold. Combining this trend with the effect of the volatile species acting on intervals 1B to 3B only, we will here see a higher conductivity with temperature. These two effects together might explain the levels in conductivity we see in Figure 42. (The weight of each effect is unknown.)

If the volatile species are dominating in the conductivity record during the Eemian–Early glacial period, a lower chloride level compared to the normal Na^+/Cl^- ratio would be present due to the reaction described above. Therefore it would be interesting to have had the chloride (or nitrate) record to check if this is actually true or not.

6.3 Mean levels of impurities - Eemian versus Holocene

As it has turned out, annual layers in the Eemian period are hard to identify. Some components are smoothed out, and some might just show noise instead of seasonal variability, but if we assume that the amounts of impurities from deposition are kept the same even at this depth, I would, as described earlier, expect the concentration levels to be more extreme in the Eemian ice than the Holocene ice. By this I mean that when the temperature is higher, I would in the direct temperature dependent components expect more impurities in the Eemian ice, and in the inversely temperature dependent components expect fewer impurities in the Eemian ice. This has shown not to be the case. Ammonium does, as expected, show a higher concentration level with temperature, but the level of interval 3B is not above the level of interval 1A. Also the dust level for interval 3B does not go below the level for interval 1A. And finally the conductivity level, with an apparently direct temperature dependency in interval 1B to 3B does not have a interval 3B level higher than the interval 1A level either.

All this together shows that the concentration levels are not more extreme in the Eemian ice although the temperature is about 5 degrees higher at this point. This might be due to diffusion processes in the ice at this depth, the fact that only 2.2m of ice in each section is measured, or that the Eemian interglacial simply had different atmospheric aerosol loads compared

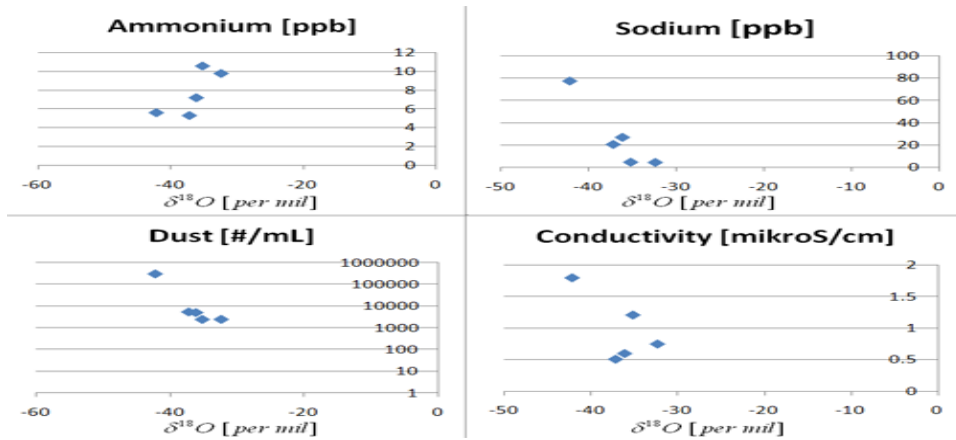


Figure 44: A plot of the mean levels of impurities with the $\delta^{18}O$ values. The data points are seen not to be on a perfect line.

to the Holocene. In this case the impurity loads are not linearly temperature dependent, so what can we then expect if the global temperature during the next hundred years rises with several degrees? It might seem as if the aerosol load would reach some sort of saturation level. See Figure 44 for a plot of the mean levels of impurities with $\delta^{18}O$. The data points are seen not to be on a perfect line.

The IPCC predicted temperature rise also has other sources than the higher temperature during the Eemian so the impurities will probably respond differently.

6.4 Resolution of NGRIP compared to GRIP records

Figure 45 shows a comparison of the power spectra from previous measurements of GRIP Ca^{2+} and GRIP NH_4^+ together with the power spectrum of my NH_4^+ results.

According to Rasmussen et al. 2005 [Rasmussen, 2005], where a deconvolution method for CFA profiles is presented, a difference between the least squares fit to the signal, P_{signal} (turquoise), and to the noise, P_{noise} (grey), can be identified in a fourier spectrum. This is done by minimizing the total RMS²⁰ difference between the sum of P_{signal} and P_{noise} and the actual spectrum. The intersection between these two lines will then suggest the maximum resolution of annual layer thicknesses. As seen in the figure, the

²⁰Root Mean Square

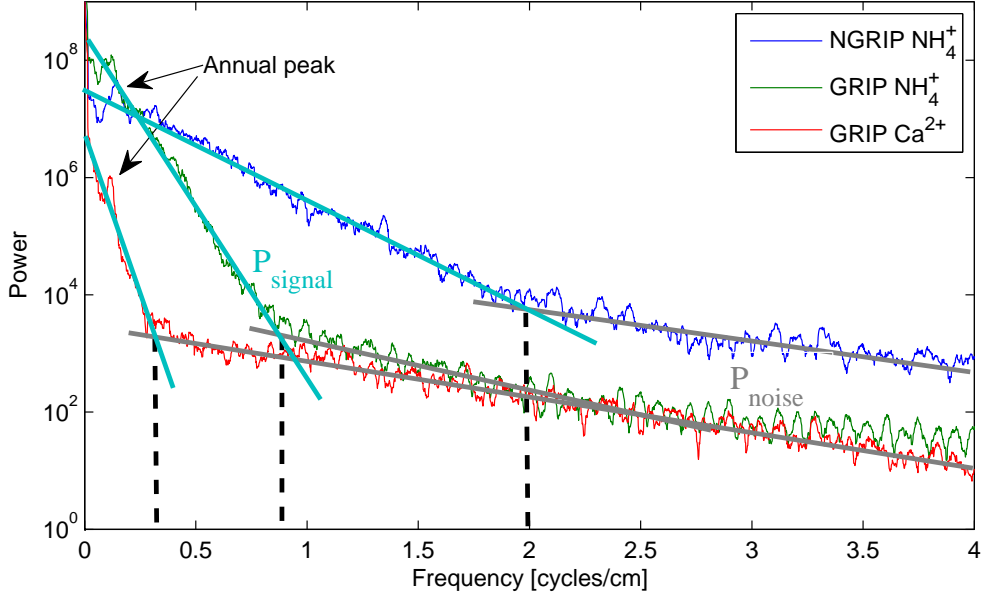


Figure 45: A power spectrum of ammonium from NGRIP, ammonium from GRIP, and calcium from GRIP from corresponding depth intervals (NGRIP: 1383.80m – 1389.30). The annual peak is shown. The intersection between P_{signal} and P_{noise} describes the maximum resolution in each component as indicated by the vertical dashed lines.

GRIP data has a steeper declination in the beginning and therefore does not have as good a resolution which is indicated by the vertical lines at the intersection of P_{signal} and P_{noise} in the spectra. These results were used during my measurement period to predict whether we were going to be able to detect Eemian layers, if present, and the results showed a resolution of approximately $\frac{1cm}{2yr}$ ($\sim 2\frac{cycles}{cm}$ see Figure 45), so we would probably be able to detect annual layers.

6.5 Neutralization of the ice

Figure 31 on page 42 shows a comparison between ammonium and ECM (plotted on a log-reverse scale) and between ECM and conductivity. Sodium is left out. A correlation is seen in the comparison of ammonium peaks and ECM lows. I have shown the ECM data on a log scale and reversed it so that peaks in ammonium correspond to peaks in ECM. The depth

scale of the ECM record can be a little off due to the uncertainty in ECM measurements. As ECM is measured with electrodes simply drawn along a surface, it produces uncertainties in the exact depth of the measurement. We see some similarity in the two components although not enough to say that it is clearly visible.

If we look at the Eemian and Early glacial intervals, this correlation between ammonium and ECM is still seen even though the ammonium in this time period seems to be smoothed out. (See Figure 46 and Figure 47). This indicates that there could be a correlation between the two records.

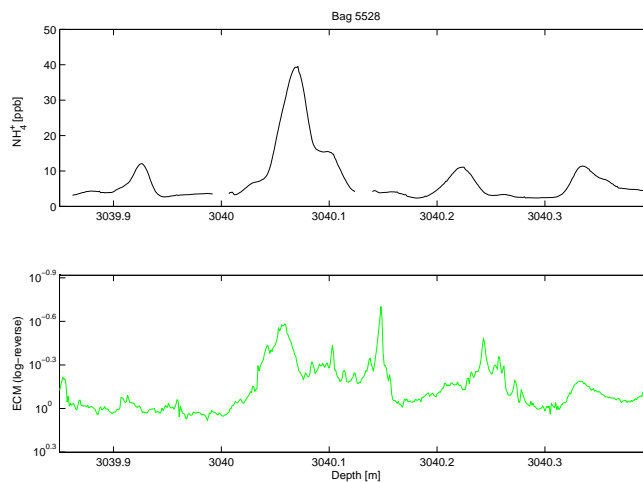


Figure 46: A comparison between ECM and ammonium for bag 5528. Note that ECM is plotted on a reversed logarithmic scale. A distinct similarity is seen in the low frequency variability.

The ECM signal is thought to be controlled primarily by the acidity of the ice, but studies have shown that there may also exist a secondary effect from the accompanying anion [Wolff, 1997]. Figure 48 shows the ECM signal and ammonium concentration across a section of the GRIP core. The drop in ECM when ammonium blows up is recognized. Maybe in some peaks the acidity of the ice has been reduced due to neutralization, but a more reasonable explanation would be that the H^+ ions are partly unavailable due to their association with the weak acid anions like formate (HCOO^-) and acetate (CH_3COO^-). These anions usually accompany the biomass burning events from which the ammonium is produced.

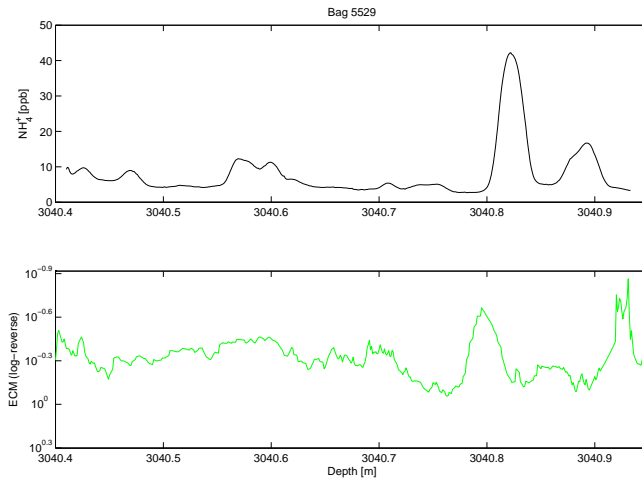


Figure 47: A comparison between ECM and ammonium for bag 5529. Note that ECM is plotted on a reversed logarithmic scale. A distinct similarity is seen in the low frequency variability.

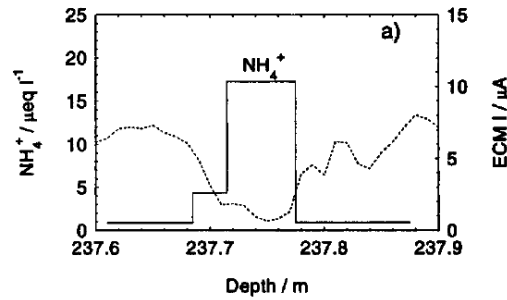


Figure 48: Plot of NH_4^+ and ECM from Wolff et al. [Wolff, 1997]. The ammonium signal is from a high-concentration event that has been ascribed to the arrival of biomass burning plume at the site ([Wolff, 1997] Fig.2a)

Crystal boundaries

Figure 15 on page 20 shows a comparison of the line scan images from the Eemian ice (*i*) as well as the Holocene ice (*a*) and ice in between. A remarkable difference is seen. Where the Holocene ice shows some layering, although nearly transparent [Svensson, 2005], the Eemian ice has no such thing. It mostly consists of crystal boundaries, but not far into the glacial

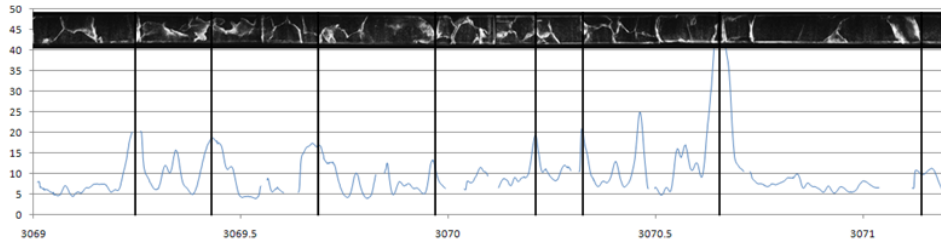


Figure 49: A comparison of ammonium peaks with crystal boundaries as seen on linescan images for interval 3B. Vertical lines indicate where some similarity is seen.

clear annual layers, caused by dust, are seen (see Figure 15 (*h*) on page 20). As the line scan is performed on a 3cm thick slab of ice, it might not resolve layering if this is just a little bit inclined compared to the depth direction.

An explanation of the ammonium signal from the intervals 1B to 3B can perhaps be found by looking at the visual stratigraphy for the depths in question. The ammonium is surely smoothed out, but it still has some large peaks once in a while. Figure 49 shows a comparison between the line scan images and the ammonium record for interval 3B (see Appendix B for interval 1B and 2B results). The line scan images clearly show large ice crystals, but as the method only gives the view from one side, it will not show every crystal boundary in the ice. It is rather difficult to say whether there exists a clear correlation between ammonium peaks and crystal boundaries or core breaks, but one might say that the big peaks correlate with some of the boundaries in the ice. (The core probably breaks at crystal boundaries since it is more fragile here, and therefore the breaks should also be taken into account when comparing to ammonium peaks.)

6.6 Improvements of the setup

Adjustments during the measurements

During measurements we experienced quite a lot of problems. At first the ice core was not aligned very well on the melting device due to smaller ice dimensions than anticipated, and this could have caused contamination from the outer parts of the ice section. A small adjustment piece was inserted, and for the Eemian–Early glacial cores a new melting device was made. Still the inner dimensions of the melting head were the same, but the core was

now aligned again. Contamination was also present in the beginning and end of an ice section but mainly due to cutting the ends of with a saw. This is difficult to avoid without spending a lot of time cleaning the ends with a microtome knife.

At breaks in the ice, contamination often occurred and was very prominent in the dust measurements. To avoid this, the breaks were cut away before measurement so that no contaminated ice went through the system. This means that a lot of data was lost, but it prevented the dust record from having a tail of contamination along with it. The contamination often consisted of drilling liquid that finds its way into the core where this is broken.

A problem during measurements, which did not have a big influence on the end results but still is very annoying to have to deal with, is air bubbles. They come from the ice, from the blank water, develop in the debubbler, develop in the joints, and maybe also in other parts. It is pretty laborious to manually remove these air bubbles, but it is required to get a nice impurity profile. It would be better if they did not exist in the first place. This means optimizing the debubbler so that it actually removes all air bubbles from the ice. This is done by avoiding it getting dirty on the inside because air bubbles like to stick to the dirt and build up to very large bubbles that are released further into the system. Also the debubbler itself should not produce air bubbles which is ensured when the construction is tight enough in all joints.

Often the problems with air occurred during standard measurements, especially when measuring blank. This leads me to think that the bubbles somehow are dissolved gases in the blank water, and when this blank water runs through the system, the bubbles are released. This problem could maybe be solved by inferring a vacuum pressure onto the blank water so that air and tiny bubbles in the water are removed.

Future improvements

As the CIC setup is almost an exact copy of the KUP setup with regard to things like chemicals, tubing and flow rate, it would be interesting to play around with these parts of the system. A check of the different reagent concentrations could for instance be made (old formulas for reagents are used right now (pers. comm. M. Bigler)), and whether shorter mixing coils would improve the resolution of the signals. The detection limit should be maintained as well as the signal to noise ratio; or at least they should not be worse. Maybe the coiled tubing used for warming up and cooling down the

ammonium sample water is longer than necessary. I would imagine that this could be an easy test to run and a quick way to reduce some tubing length and hence avoid dispersion in this section.

As I am informed, no other pump rate setting than 0.9mL/min for the peristaltic pump is used, so this could be played around with. If the pump rate is changed, the tubings also have to be changed since the inner dimensions of these should fit together with the pump rate. When measuring sodium an absorbance method is used. It would be interesting to look around for for instance a way to measure sodium with fluorescence spectroscopy as we do with ammonium. This approach is much easier and simple, and it might therefore enhance the resolution of the signal. Finally an “open” debubbler would be an idea to work with. This open debubbler is an easy way of releasing excess pressure in the system which might help the drifting baselines and negative values in sodium, but it might also cause a risk of losing temporal resolution due to the required usage of a melting pump. A sketch of such an open debubbler is shown on Figure 50.

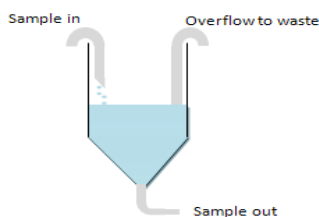


Figure 50: A simple sketch of the debubbler used with the KUP setup. The principle of the debubbler is a dripping water sample into a small pipette, and an overflow to waste. The sample is then collected from the bottom of the pipette wherefrom air bubbles in the sample water should have raised to the surface and dissolved.

7 Conclusion

During this study CFA profiles from the NGRIP ice core section from 1378.30m–1389.30m, as well as from the depths 2995.30–2997.50m, 3039.85–3042.05m, and 3069.00 – 3071.20m have been obtained. A new CFA setup was used which involved a couple of technical issues. The sodium instrument had problems with a drifting baseline which also was too high in concentration and hence produced negative values.

Besides this, the setup worked quite well except for small problems that were adjusted for in the data processing. The resolution of the setup was seen to be very good, as anticipated. According to a spectral fourier analysis, the setup would be able to detect annual layers down to a thickness of around $0.5 \frac{cm}{year}$ which meant that Eemian annual layers, if present, could be identified.

A dating of the Holocene period was obtained, and this dating matched the existing GICC05 dating well; the GICC05 has 146 years in the measured 11m of Holocene ice, and I have counted 145 ± 1 years. A dating of the Eemian–Early glacial intervals was also made. This more questionable result was compared to the modelled annual layer thickness from the ss09sea model. Although the dust and conductivity results from this period (that were the only two components where seasonal variation was identified) only showed annual layers weakly, an estimate of annual layer thickness fitted to some degree with the ss09sea model; at least for interval 1B and 2B. Here an annual layer thickness of around $0.97 \frac{cm}{year}$ was found.

Interval 3B, on the other hand, showed a smaller annual layer thickness than predicted by ss09sea, $1.12 \frac{cm}{year}$ compared to $1.47 \frac{cm}{year}$, and if my dating is correct, this means that 328 years more (estimated from the bottom 16m of the ice core) from the Eemian period are located in the NGRIP ice core than modelled.

Finally the mean levels of the atmospheric aerosol loads, contained in the ice core in the different climatic periods, were compared. The Eemian, although 5 degrees warmer than the Holocene, did not show the more extreme values that were expected. This might suggest that although the chemical components depend on temperature, this is not a linear dependency. On the other hand it might simply indicate an effect of diffusion processes.

Further work

- An obvious next step would be to improve the setup in general. This includes increasing the sensitivity of sodium, for instance by constructing temperature stabilization boxes for all components but most importantly for sodium. Besides this, an excess pressure release should be added, maybe in form of an open debubbler and together with this, the resolution of the setup could be enhanced by doing tests with shorter mixing coils or adjusting the reagents solutions to improve sensitivity as well.
- In the future, more components could also be added to the CIC CFA setup, for instance SO_4^{2-} and Ca^{2+} . This unfortunately will decrease the temporal resolution of the setup.
- Finally, tuning the bottom melting parameters in the ss09sea model would be interesting to see if annual layer thicknesses, as found in this thesis, can be achieved.

8 Danish summary — Dansk resumé

Metoden *Continuous Flow Analysis*, CFA, bruges til målinger af kemiske urenheder, uopløseligt støv og den elektrolytiske ledningsevne for smeltet is, *konduktivitet*. Metoden benyttes til at opnå højt opløselige optegnelser over sæsonvariationelle klimaproxier fra fortiden. CFA udføres ved at placere en 55cm lang issektion med et tværsnit på 34mm×34mm vertikalt ovenpå et smeltehoved. Herfra smeltes isen og analyseres med forskellige apparater, som inkluderer bla. fluorescens- og absorptionsspektroskopi. Jeg har i dette speciale koncentreret mig om følgende komponenter; ammonium, som er en indikator for processer af biologisk oprindelse, natrium, som kommer fra det marine miljø, uopløseligt støv, som bliver transporteret til Grønland pga. ørkenstorme og endelig konduktivitet, som er et samlet signal over de forskellige kemiske urenheder.

Jeg har i løbet af mit speciale opnået CFA profiler fra 4 sektioner af *North Greenland Ice Sheet Project*, NGRIP, iskernen. En sektion er fra den nuværende mellemistid, Holocæn, fra dybden 1373,80m – 1389,30m. De 3 sidste er fra den sidste mellemistid, Eem, fra transitionen til istid, og endelig en fra starten af istiden fra *Dansgaard-Oeschger event 25*, DO-25. Disse sektioner er henholdsvis fra dybderne 3069,00m – 3071,20m, 3039,85m – 3042,05 og 2995,30m – 2997,50m.

Støvmålingerne viste sig at have ret forskellige middelværdier i forhold til tidligere målinger. Forklaringen er ikke umiddelbart ligetil, men det er sandsynligvis et spørgsmål om målemetode eftersom selve profilerne udviser god sæsonvariation på trods af til tider udbredt kontaminering. Ligeså har natrium vist sig at have pæn sæsonvariation på trods af problemer med negative koncentrationstværdier og en hældende referenceniveau. Middelværdierne for alle fire komponenter har vist sig at være ikke-lineære i forhold til temperatur, selvom de alle fire har en stærk temperaturafhængighed.

Dateringen af Holocæn-issektionen har vist sig at stemme godt overens med den eksisterende tidsskala GICC05; hvor GICC05 har dateret 146år har jeg talt 145 ± 1år. En forskel findes dog i min datering af issektionen fra Eem-perioden i forhold til ss09sea-modellen. Min middelårlagstykkelse er 0.35 $\frac{cm}{år}$ mindre end den modellerede årlagstykkelse. Denne forskel resulterer i 328år ekstra af Eem-perioden i de nederste 16m af NGRIP iskernen.

Endelig er forslag om implementering af en sulfat- og kalciumkomponent fremført, ligesåvel som forbedringer af debubbleren og natriumsignalet bør tilstræbes.

A Greenland interstadials

Figure 51 shows the NGRIP isotopic profile from around 75ka to 123ka. Numbers indicated above the profile refer to Dansgaard-Oeschger, DO, events, and numbers indicated below indicate Greenland Stadial, GI, events. My interval 1B is from DO-25.

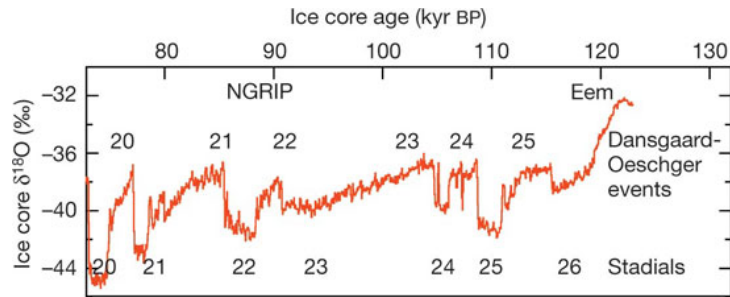


Figure 51: The NGRIP isotopic profile with indications of Greenland interstadials including DO25 [NGRIP members, 2004].

B Additional results

Holocene CFA results

Figures 52, 53, and 54, show my CFA profiles from bag 2507-2511, 2517-2521, and 2522-2526 respectively.

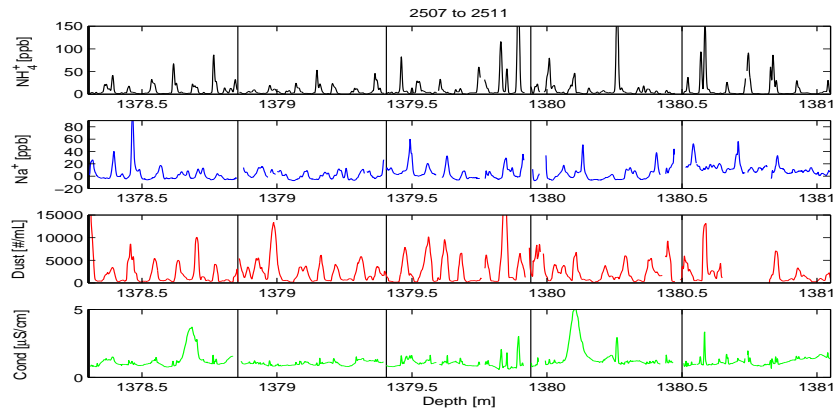


Figure 52: CFA profile of bag 2507 to 2511 (Depth interval: 1378.30m – 1381.05m). Vertical lines indicate separation of bags.

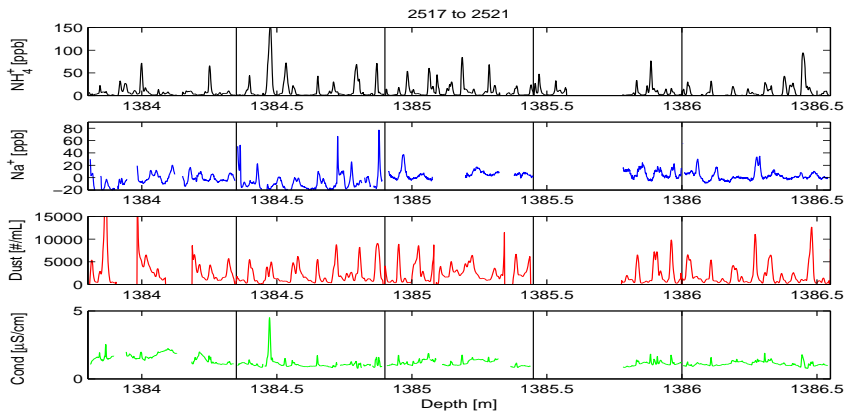


Figure 53: CFA profile of bag 2517 to 2521 (Depth interval: 1383.80 – 1386.55m). Vertical lines indicate separation of bags.

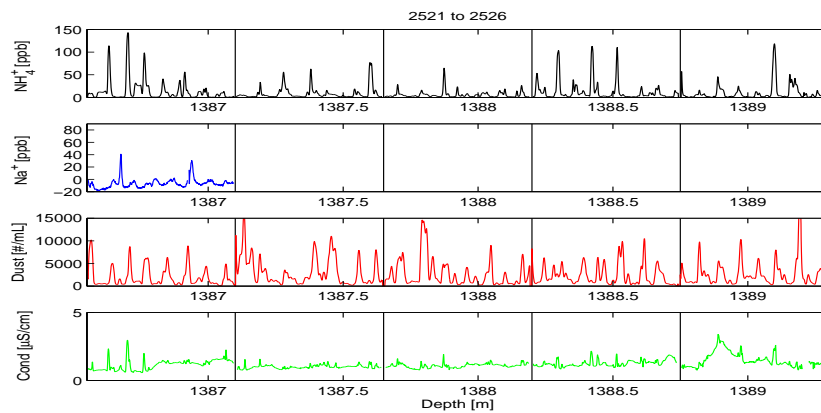


Figure 54: CFA profile of bag 2521 to 2526 (Depth interval: 1386.55 – 1389.30m). Vertical lines indicate separation of bags.

Crystal boundaries and ammonium

Figures 55 and 56 show my comparisons of the ammonium record with the line scan images for my intervals 1B and 2B.

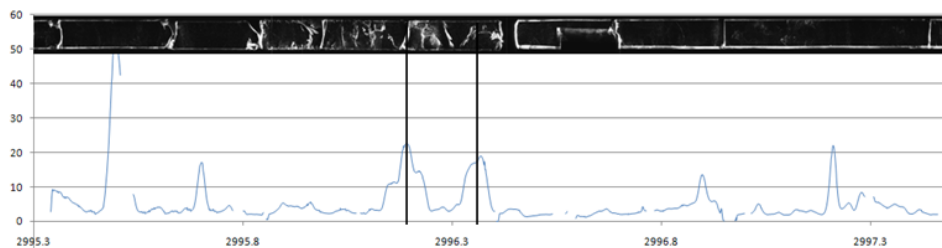


Figure 55: A comparison of ammonium peaks with crystal boundaries as seen on linescan images. Vertical lines indicate where some similarity is seen.

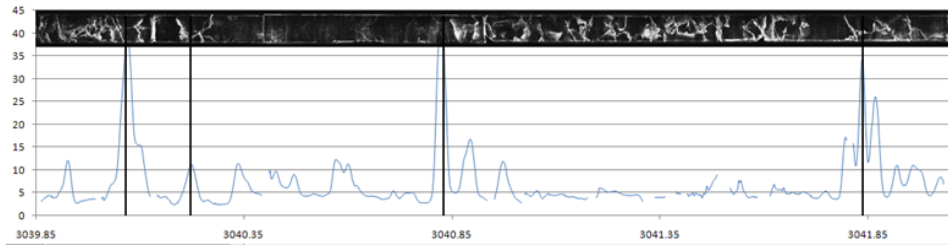


Figure 56: A comparison of ammonium peaks with crystal boundaries as seen on linescan images. Vertical lines indicate where some similarity is seen.

List of Figures

1	Map of Greenland	2
2	$\delta^{18}\text{O}$ profile	3
3	The setup	5
4	Box of ice	6
5	Flow in ice sheet	7
6	NGRIP CFA profile 1404m to 2930m	10
7	NGRIP CFA profile 1405m to 1406m	10
8	GICC05 overview	12
9	Comparison of ss09sea and GICC05	13
10	ss09sea	13
11	Sodium concentrations over last glacial cycle	15
12	Microparticle concentrations	17
13	Cutting plan	18
14	Air close off	19
15	Line scan images	20
16	Schematic drawing of ECM	21
17	$\delta^{18}\text{O}$ and annual layer thickness	22
18	$\delta^{18}\text{O}$ incl. intervals	23
19	Schematic overview of setup	25
20	Melting device	26
21	Energy states	28
22	Absorption technique	29
23	Sodium calibration	30
24	Temporal resolution NH_4^+ and conductivity	33
25	Resolution plots	34
26	Spatial resolution plot - different flow rate	35
27	Spatial resolution plot - same flow rate	36

28	Raw data plot	39
29	Processed data plot	40
30	CFA profile bag 2512 to 2516	41
31	ECM comparison	42
32	Power spectrum bags 2517 to 2526	44
33	Plot of dating and phasing of components	44
34	Raw data plot of sodium	45
35	Sodium after adjustment	47
36	Interval 1B profile	49
37	Interval 2B profile	49
38	Interval 3B profile	50
39	Conductivity and dust	51
40	mQ ice and blank versus conductivity signal	52
41	Power spectrum of interval 1B	53
42	Concentration levels	56
43	Insolation plot	58
44	Temperature dependency	60
45	Power spectrum comparison - NGRIP, GRIP	61
46	ECM and ammonium 1	62
47	ECM and ammonium 2	63
48	Plot of ammonium and ECM from Wolff et al.	63
49	Crystal boundaries	64
50	Debubbler	66
51	Greenland interstadials	70
52	CFA profile from bag 2507 to 2511	71
53	CFA profile from bag 2517 to 2521	71
54	CFA profile from bag 2521 to 2526	72
55	Crystal boundaries and ammonium 1	72
56	Crystal boundaries and ammonium 2	73

List of Tables

1	Annual layer counting - Holocene	45
2	Means and medians - KUP vs CIC	46
3	Annual layer counting - Eemian and Early glacial	53
4	Mean levels of the four components	57

References

- [ACS Comm 1980] ACS Committee on Environmental Improvement *Guidelines for Data Acquisition and Data Quality Evaluation in Environmental Chemistry* Anal. Chem. 52, 2242-2249, 1980
- [Andersen, 2006] K.K. Andersen, A. Svensson, S.J. Johnsen, S.O. Rasmussen, M. Bigler, R. Röthlisberger, U. Ruth, M.-L. Siggaard-Andersen, J.P. Steffensen, D. Dahl-Jensen, B.M. Vinther, H.B. Clausen *The Greenland Ice Core Chronology 2005, 15-42ka. Part 1: constructing the time scale* Quaternary Science Reviews 25 (2006) 3246-3257
- [Berg-Sørensen, 2004] K. Berg-Sørensen, H. Flyvbjerg *Power spectrum analysis for optical tweezers* Review of scientific instruments, Vol 75, num 3, 2004
- [Bigler, 2007] M. Bigler, A. Svensson, J.P. Steffensen, P. Kaufmann *A new continuous high-resolution detection system for sulphate in ice cores* Annals of Glaciology 45, 2007
- [Busenbergl, 1979] E. Busenbergl and C.C. Langway Jr. *Levels of Ammonium, Sulfate, Chloride, Calcium, and Sodium in Snow and Ice From Southern Greenland* Journal of Geophysical Research, Vol 84, NO. C4, 1979
- [Dansgaard et al. 1969] W. Dansgaard, L. Merlivat, and E. Roth *Stable isotope measurements on firn cores* Meddelelser om Grønland, 177(2):62-76
- [Drysdale, 2007] R.N. Drysdale, G. Zanchetta, J.C. Hellstrom, A.E. Fallick, J. McDonald, I. Cartwright *Stalagmite evidence for the precise timing of North Atlantic cold events during the early glacial* Geology, January 2007: v.35;no.1;p.77-80
- [EPICA 2004] EPICA community members *Eight glacial cycles from an Antarctic ice core* Nature Vol 429, 2004
- [Fischer, 2007] H. Fischer, M.L. Siggaard-Andersen, U. Ruth, R. Röthlisberger, E. Wolff *Glacial/Interglacial changes in mineral dust and sea-salt records in polar ice cores: sources, transport, and deposition* Reviews of Geophysics, 45, 2007
- [Fuhrer, 1996] K. Fuhrer, A. Neftel, M. Anklin, T. Staffelbach, M. Legrand *High-resolution ammonium ice core record covering a complete glacial-interglacial cycle* Journal of Geophysical Research, Vol. 101, NO. D2, P:4147-4164, 1996

- [Fuhrer, 1997] K. Fuhrer and M. Legrand *Continental biogenic species in the Greenland Ice Core Project ice core: Tracing back the biomass history of the North American continent* Journal of Geophysical Research, Vol. 102, NO. C12, P:26,735-26,745, 1997
- [Genfa, 1989] Z. Genfa and P.K. Dasgupta *Fluorometric Measurement of Aqueous Ammonium Ion in a Flow Injection System* Anal. Chem., 61, 408-412
- [Harsham 1995] K.D. Harsham *Water sampling for pollution regulation* Environmental Technology Series, Vol. 1, Gordon & Breach, 1995
- [IPCC, 2007] S. Solomon, D. Qin, M. Manning, Z. Chen, M. Marquis, K.B. Averyt, M. Tignor and H.L. Miller *IPCC Fourth Assessment Report, Climate Change 2007: The Physical Science Basis - Chapter 1* Cambridge University Press, 2007
- [Johnsen, 2001] S.J. Johnsen, D. Dahl-Jensen, N. Gundestrup, J.P. Steffensen, H.B. Clausen, H. Miller, V. Masson-Delmotte, A.E. Sveinbjornsdottir, J. White *Oxygen isotope and palaeotemperature records from six Greenland ice-core stations: Camp Century, Dye-3, GRIP, GISP2, Renland and NorthGRIP* Journal of Quaternary Science, 16, 299-307, 2001
- [Kaufmann, 2008] P.R. Kaufmann, U. Federer, M.A. Hutterli, M. Bigler, S. Schüpbach, U. Ruth, J. Schmitt, T.F. Stocker *An improved Continuous Flow Analysis (CFA) system for high-resolution field measurements on ice cores* Environ. Sci. Technol., 42(21), 8044-8050, 2008
- [Landais, 2006] A. Landais, V. Masson-Delmotte, J. Jouzel, D. Raynaud, S. Johnsen, C. Huber, M. Leuenberger, J. Schwander, B. Minster *The glacial inception as recorded in the NorthGRIP Greenland ice core: timing, structure and associated abrupt temperature changes* Climate Dynamics 26, 273-284, 2006
- [Legrand, 1992] M. Legrand, M. Angelis, T. Staffelbach, A. Neftel, B. Stauffer *Large perturbations of ammonium and organic acids content in the Summit-Greenland ice core. Fingerprint from forest fires?* Geophysical Research Letters, Vol 19, No 5, P:473-475, 1992
- [Mayewski, 1987] P.A. Mayewski, M.J. Spencer, Wm.B. Lyons, M.S. Twickler *Seasonal and spatial trends in South Greenland snow chemistry* Atmospheric Environment, Vol. 21, No. 4, P:863-869, 1987

- [Moore, 1994] J.C. Moore, E.W. Wolff, H.B. Clausen, C.U. Hammer, M.R. Legrand, K. Fuhrer *Electrical response of the Summit-Greenland ice core to ammonium, sulphuric acid, and hydrochloric acid* Geophysical Research Letters, Vol 21, No. 7, P:565-568, 1994
- [NGRIP members, 2004] NGRIP members *High-resolution record of Northern Hemisphere climate extending into the last interglacial period* Nature, Vol 431, 2004
- [Quilles, 1993] R. Quilles, J.M. Fernandez-Romero, E. Fernandez, M.D. Luque de Castro, M. Valcarcel *Automated Enzymatic Determination of Sodium in Serum* Clinical Chemistry, Vol 39, No 3, 1993
- [Rasmussen, 2005] S.O. Rasmussen, K.K. Andersen, S.J. Johnsen, M. Bigler, T.McCormack *Deconvolution-based resolution enhancement of chemical ice core records obtained by Continuous Flow Analysis* Journal of Geophysical Research, 2005
- [Rasmussen, 2006] S.O. Rasmussen, K.K. Andernse, A.M. Svensson, J.P. Steffensen, B.M. Vinther, H.B. Clausen, M.-L. Siggaard-Andersen, S.J. Johnsen, L.B. Larsen, D. Dahl-Jensen, M. Bigler, R. Röthlisberger, H. Fischer, K. Goto-Azuma, M.E. Hansson, U. Ruth *A new Greenland ice core chronology for the last glacial termination* Journal of Geophysical Research, 2006
- [Rasmussen, 2007] S.O. Rasmussen, B.M. Vinther, H.B. Clausen, K.K. Andersen *Early Holocene climate oscillations recorded in three Greenland ice cores* Quaternary Science Reviews 26, 1907-1914, 2007
- [Ruth, 2002] U. Ruth, D. Wagenbach, M. Bigler, J.P. Steffensen, R. Röthlisbergern, H. Miller *High resolution microparticle profiles at NGRIP: case studies of the calcium - dust relationship* Annals of Glaciology 35, 2002
- [Ruth, 2003] U. Ruth, D. Wagenbach, J.P. Steffensen, M. Bigler *Continuous record of microparticle concentration and size distribution in the central Greenland NGRIP ice core during the last glacial period* Journal of Geophysical Research, Vol 108, No D3, 2003
- [Ruth, 2008] U. Ruth, C. Barbante, M. Bigler, B. Delmonte, H. Fischer, P. Gabrielli, V. Gaspari, P. Kaufmann, F. Lambert, V. Maggi, F. Marino, J.-R. Petit, R. Udisti, D. Wagenbach, A. Wegner, E.W. Wolff *Proxies*

and Measurement Technique for Mineral Dust in Antarctic Ice Cores Environ. Sci. Technol. 42(15), 5675-5681, 2008

- [Röthlisberger, 2000] R. Röthlisberger, M. Bigler, M. Hutterli, S. Sommer, B. Stauffer *Technique for Continuous High-Resolution Analysis of Trace Substances in Firn and Ice Cores* Environ. Sci. Technol. 34(2), P: 338-342, 2000
- [Schwander, 1996] J. Schwander *Gas diffusion in firn, in Chemical Exchange Between the Atmosphere and Polar Snow*, edited by E. W. Wolff and R. C. Bales, pp. 527-540, 1996
- [Sigg, 1994] A. Sigg, K. Fuhrer, M. Anklin, T. Staffelbach, D. Zurmuehle *A continuous analysis technique for trace species in ice cores* Environ. Sci. Technol. 28(2), 204-209, 1994
- [Steffensen, 1997] J.P. Steffensen *The size distribution of microparticles from selected segments of the Greenland Ice Core Project ice core representing different climate periods* Journal of Geophysical Research, Vol 102, No C12, P:26,755-26,763, 1997
- [Svensson, 2005] A. Svensson, S.W. Nielsen, S. Kipfstuhl, S.J. Johnsen, J.P. Steffensen, M. Bigler, U. Ruth, R. Rötliberger *Visual stratigraphy of the North Greenland Ice Core Project (NorthGRIP) ice core during the last glacial period* Journal of Geophysical Research, Vol 110, 2005
- [Svensson, 2006] A. Svensson, K.K. Andersen, M. Bigler, H.B. Clausen, D. Dahl-Jensen, S.M. Davies, S.J. Johnsen, R. Muscheler, S.O. Rasmussen, R. Röthlisberger, J.P. Steffensen, B.M. Vinther *The Greenland Ice Core Chronology 2005, 15-42ka. Part 2: comparison to other records* Quaternary Science Reviews 25, 3258-3267, 2006
- [Svensson, 2008] A. Svensson, K.K. Andersen, M. Bigler, H.B. Clausen, D. Dahl-Jensen, S.M. Davies, S.J. Johnsen, R. Muscheler, F. Parrenin, S.O. Rasmussen, R. Röthlisberger, I. Seierstad, J.P. Steffensen, B.M. Vinther *A 60.000 year Greenland stratigraphic ice core chronology* Clim. Past 4, 47-57, 2008
- [Vinther, 2006] M. Vinther, H.B. Clausen, S.J. Johnsen, S.O. Rasmussen, K.K. Andersen, S.L. Buchardt, D. Dahl-Jensen, I.K. Seierstad, M.-L. Siggaard-Andersen, J.P. Steffensen, A. Svensson *A synchronized dating of three Greenland ice cores throughout the Holocene* Journal of Geophysical Research, 2006

- [Walker, 2007] . Walker and J. Lowe *Quaternary science 2007: a 50-year retrospective* Journal of Geological Society, Vol 164, P:1073-1092, 2007
- [Wolff, 1997] E.W. Wolff, W.D. Miners, J.C. Moore, J.G. Paren *Factors Controlling the Electrical Conductivity of Ice from the Polar Regions - A Summary* J. Phys. Chem., 101, 6090-6094, 1997
- [Xia, 2007] X. ZhiFeng, K. XingGong, J. XiuYang, C. Hai *Precise dating of East-Asian-Monsoon D/O events during 95-56 ka BP: Based on stalagmite data from Shanbao Cave at Shennongjia, China* Sci China D-Earth Sci, vol 50, no 2, 228-235, 2007
- [Centre for Ice and Climate, 2009] Facts about drillings.
http://www.iceandclimate.nbi.ku.dk/research_preliminary/hojrebokse_research/drillingmap/ (Site not public yet, but we are working on it :))